Geobiology

Geobiology (2013) DOI: 10.1111/gbi.12042

Bacterial abundance and composition in marine sediments beneath the Ross Ice Shelf, Antarctica

S. A. CARR,[1] S. W. VOGEL,[2,3,4] R. B. DUNBAR,[5] J. BRANDES,[6] J. R. SPEAR,[7] R. LEVY,[8] T. R. NAISH,[9] R. D. POWELL,[2] S. G. WAKEHAM[6] AND K. W. MANDERNACK[1,10]

[1]*Department of Chemistry and Geochemistry, Colorado School of Mines, Golden, CO, USA*
[2]*Department of Geology and Environmental Geosciences, Northern Illinois University, Dekalb, IL, USA*
[3]*Australian Antarctic Division, Kingston, Tas., Australia*
[4]*Antarctic Climate & Ecosystems Cooperative Research Centre, University of Tasmania, Hobart, Tas., Australia*
[5]*Department of Environmental Earth Systems Science, Stanford University, Stanford, CA, USA*
[6]*Skidaway Institute of Oceanography, Savannah, GA, USA*
[7]*Department of Civil and Environmental Engineering, Colorado School of Mines, Golden, CO, USA*
[8]*Geological and Nuclear Sciences, Wellington, New Zealand*
[9]*Antarctic Research Centre, Victoria University, Wellington, New Zealand*
[10]*Department of Earth Sciences, Indiana University – Purdue University Indianapolis, Indianapolis, IN, USA*

ABSTRACT

Marine sediments of the Ross Sea, Antarctica, harbor microbial communities that play a significant role in the decomposition, mineralization, and recycling of organic carbon (OC). In this study, the cell densities within a 153-cm sediment core from the Ross Sea were estimated based on microbial phospholipid fatty acid (PLFA) concentrations and acridine orange direct cell counts. The resulting densities were as high as 1.7×10^7 cells mL^{-1} in the top ten centimeters of sediments. These densities are lower than those calculated for most near-shore sites but consistent with deep-sea locations with comparable sedimentation rates. The $\delta^{13}C$ measurements of PLFAs and sedimentary and dissolved carbon sources, in combination with ribosomal RNA (SSU rRNA) gene pyrosequencing, were used to infer microbial metabolic pathways. The $\delta^{13}C$ values of dissolved inorganic carbon (DIC) in porewaters ranged downcore from $-2.5‰$ to $-3.7‰$, while $\delta^{13}C$ values for the corresponding sedimentary particulate OC (POC) varied from $-26.2‰$ to $-23.1‰$. The $\delta^{13}C$ values of PLFAs ranged between $-29‰$ and $-35‰$ throughout the sediment core, consistent with a microbial community dominated by heterotrophs. The SSU rRNA gene pyrosequencing revealed that members of this microbial community were dominated by β-, δ-, and γ-Proteobacteria, Actinobacteria, Chloroflexi and Bacteroidetes. Among the sequenced organisms, many appear to be related to known heterotrophs that utilize OC sources such as amino acids, oligosaccharides, and lactose, consistent with our interpretation from $\delta^{13}C_{PLFA}$ analysis. Integrating phospholipids analyses with porewater chemistry, $\delta^{13}C_{DIC}$ and $\delta^{13}C_{POC}$ values and SSU rRNA gene sequences provides a more comprehensive understanding of microbial communities and carbon cycling in marine sediments, including those of this unique ice shelf environment.

Received 30 August 2012; accepted 13 April 2013

Corresponding author: K. W. Mandernack. Tel.: 317-274-8995; fax: 317-274-7966; e-mail: kevinman@iupui.edu

INTRODUCTION

For more than a decade, marine sediments were thought to hold 55–85% of all microbial life (Whitman *et al.*, 1998), where they selectively degrade and recycle a continuous supply of deposited labile organic matter (OM); thus playing a major role in global carbon cycling. Recently, Kallmeyer *et al.* (2012) provided lower estimates of microbial life in deep-sea sediments of 0.9–31%. The discrepancy between these estimates is largely attributed to biased sampling efforts towards sediments located along continental shores in former studies (Whitman *et al.*, 1998; Parkes

et al., 2005). The recent inclusion of deep-sea, low biomass environments are thought to have improved abundance estimates (Hinrichs & Inagaki, 2012; Kallmeyer *et al.*, 2012), emphasizing the importance of sampling a wider range of subsurface environments with varying sedimentation rates and inputs of organic carbon (OC).

During the 2006 geological ANtarctic Geological DRILLing Project (ANDRILL), the top 1.53 m of marine sediment was retrieved from beneath the Ross Ice Shelf for microbiological and geochemical analyses. The Ross Ice Shelf is the world's largest ice shelf, covering approximately 560 000 km^2. According to the marine glacial record, the Ross Ice Shelf experiences cyclic fluctuations of ice coverage approximately every 40 000 years, ranging from thick, grounded ice shelves to open ocean (Naish *et al.*, 2009). Interpretation of the lithostratigraphy at the ANDRILL site suggests that the Ross Ice Shelf persisted throughout the Holocene, providing a rare and unique opportunity to collect deep-sea sediments that were deposited below a permanent ice shelf (Fig. 1; Falconer *et al.*, 2007). Previous studies of microbial abundances from sediments of continental margins and the open ocean indicate that margin sites generally have a larger microbial population due to larger amounts of OM (Deming *et al.*, 1992; Shipboard Scientific Party, 2003; Lipp *et al.*, 2008; D'Hondt *et al.*, 2009). However, while located on the continental shelf, the ice shelf at the ANDRILL site limits sedimentation rates (0.5 mm $year^{-1}$) and sedimentary OC content (0.18 wt%; Mckay *et al.*, 2008). It remains unclear how the quantity or quality of sedimenting OM affects living cell densities and metabolic diversity within these oligotrophic sediments. Thus, the goal of this study was to analyze and compare the microbial communities within these Antarctic sediments to other marine environments.

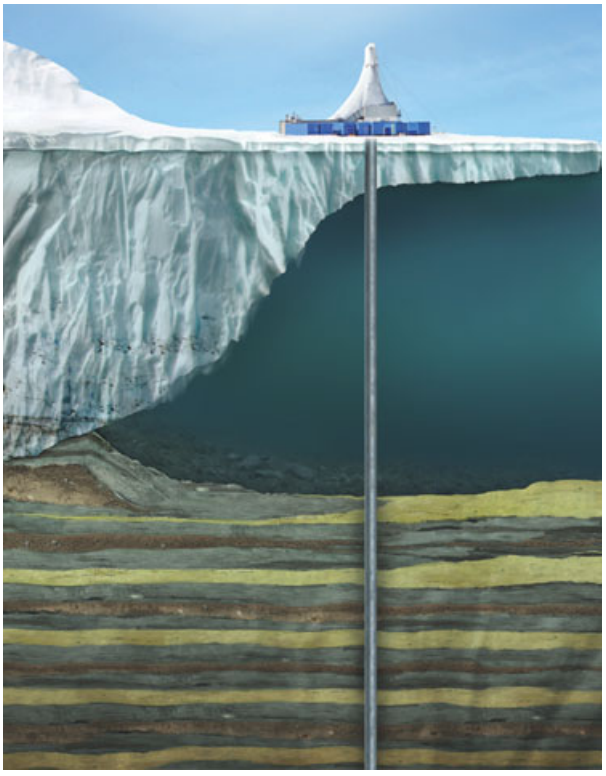

Fig. 1 A cartoon depiction of the ANDRILL Drilling Site, courtesy of the ANDRILL Program.

Understanding the effects of OM quality and quantity on the resident microbial communities requires an integrated approach that examines both the available carbon sources and indicators of microbial abundance, diversity, and metabolism. This study compares direct cell counts to estimates of viable cells based on phospholipid concentrations. Because nucleic acid stains bind to the DNA of living, dormant, and dead cells, direct counts do not always provide an accurate estimate of viable cell numbers (Smith & D'Hondt, 2006; Morono *et al.*, 2009). In addition, fluorescence from mineral grains can cause interference, increasing the error of cell estimates (Rublee, 1982). Alternatively, phospholipid fatty acid (PLFA) analyses are believed to provide an alternative means to estimate the total viable microbial population, as PLFAs degrade within weeks of cell death, and have been used to characterize microbial communities in other marine sediments (Harvey *et al.*, 1986; Summit *et al.*, 2000; Mills *et al.*, 2006; Guiilini *et al.*, 2010).

Metabolic pathways and microbial diversity were investigated by structural and stable carbon isotope analysis of PLFAs ($\delta^{13}C_{PLFA}$). In particular, the $\delta^{13}C_{PLFA}$ values provide information relating to the carbon sources and metabolic pathways utilized by the microbial community (Abraham *et al.*, 1998; Pancost & Sinninghe Damsté, 2003). Depending on the phospholipid synthetic pathway and associated ^{13}C fractionation effects, lipids produced from carbon intermediates of the various assimilation pathways will show a range of $\delta^{13}C$ values, but ultimately reflect the $\delta^{13}C$ of their carbon substrates (Londry *et al.*, 2004; Schouten *et al.*, 2004; Zhang *et al.*, 2004). Due to the complexity of environmental samples, PLFA analyses were integrated with estimates of microbial abundance, small subunit (SSU) ribosomal RNA sequencing, porewater geochemistry, $\delta^{13}C_{DIC,}$ and $\delta^{13}C_{POC}$ values. This integrated analytical approach provided a more comprehensive understanding of microbial abundance, diversity, and influences on carbon cycling in these deep-sea sediments beneath the ice shelf of the Ross Sea.

METHODS

Site description

Soft sediment cores from ANDRILL site AND-1B were collected from locations beneath the Ross Ice Shelf, which

has a thickness of 82 m, at water depths of approximately 850 m (−77°53′22″, 167°5′22″; Fig. 1). Of the four push cores recovered, three were used for geological studies while the longest (PU-010) was reserved for microbiological investigations. The cored sediments are best described as muds with occasional rounded, granule-sized clasts of mudstone, quartz and basalt with most biosiliceous material contained within the top 60 cm below sea floor (cmbsf; Dunbar *et al.*, 2007).

Sediment sample collection

All push cores were collected by attaching the push corer assembly to the end of the PQ drill bit (83 mm diameter; Dunbar *et al.*, 2007). The push corer was pressed into sediments without drilling fluids or drill rotation. Push Core 010 was pushed on October 26, 2006, to a depth of 1.53 m. Sampling methods for microbiology were modified from D'Hondt *et al.* (2003) and described by Pompilio *et al.* (2007) as briefly noted here. After drilling, the core was transferred intact to a nearby laboratory for further microbiological and geochemical subsampling in a sterile laminar flow hood. The core was extruded from the polyvinylchloride core liner, and alternating whole round cores (WRNDs) were cut with a sterile (autoclaved) spatula at 5 cm intervals for pore water chemistry and microbiological analyses. The microbiological WRNDs were then immediately subsampled by inserting a pre-sterilized 5-mL-plastic syringe barrel into the center of each WRND and withdrawing approximately 5 mL of sediment. The top and bottom 1 mL of this 5 mL subsample were preserved separately for acridine orange direct counting (AODC), and the middle 3 mL of sediment was saved for DNA analysis. The remaining WRND was dedicated to phospholipid analyses, and both the molecular and phospholipid subsamples were immediately covered and frozen on the Antarctic ice (approximately −20 °C) until transferred to a freezer in the Crary laboratory at McMurdo Station (−80 °C). The samples were subsequently shipped frozen to the Colorado School of Mines (CSM) where they were stored at −80 °C until analyzed.

Geochemistry

Whole round cores reserved for porewater analyses were compressed with titanium squeezers according to ODP sampling protocols (Manheim & Sayles, 1974) and were previously described by Dunbar *et al.* (2007). All porewater samples were immediately filtered (0.2-μm-nylon membrane filter). Porewater measurements made at the drill site included pH, alkalinity, SO_4^{2-}, O_2, and NH_4^+ (Dunbar *et al.*, 2007; Pompilio *et al.*, 2007). Dissolved oxygen concentrations were also measured at the drill site using a Mettler 4100e oxygen sensor (Mettler Toledo, Columbus, OH, USA) and an YSI dissolved oxygen meter (YSI Incorporated, Yellow Springs, OH, USA). Porewater samples for nitrate and nitrite were acidified to pH < 2 and kept refrigerated during storage (4 °C) and shipment to CSM and subsequently analyzed in Dr. Richard Smith's laboratory (U.S. Geological Survey, Boulder, CO, USA) with a chemiluminescent nitric oxide detector (Model NOA 280; GC Analytical Instruments, Boulder, CO, USA). $\delta^{13}C$ values of dissolved inorganic carbon (DIC) and particulate OC (POC) were measured at the Stable Isotope Biogeochemistry Laboratory at Stanford University. After acidification, CO_2 was evolved from DIC via acidification and cryogenic vacuum extraction and measured on a FinniganMAT 252 isotope ratio mass spectrometer (IRMS; Gruber *et al.*, 1999). Squeeze cakes were lyophilized, and sedimentary POC concentrations and $\delta^{13}C$ measurements were made using a Carlo Erba NA1500 elemental analyzer/Conflo II system coupled to a Finnigan DeltaPlus IRMS following procedures outlined in Moy *et al.* (2008). Results are presented in standard delta notation relative to the Vienna Pee Dee Belemnite (VPDB). One standard deviation was ±0.05‰ for $\delta^{13}C$ DIC and POC measurements and 0.14% for wt% POC.

Cell counts

Microbial cell counts were estimated using AODC techniques based on Hobbie *et al.* (1977). Although there are limitations and concerns with AODC for estimating cell numbers, as previously noted, they have long been used in IODP studies and in other marine environments (Parkes *et al.*, 2000, 2007; Luna *et al.*, 2002), and can thus provide some direct comparisons with these earlier studies. Furthermore, AODC was used only as one indicator of cell numbers in this study and was directly compared to estimates based on PLFA analysis (below). For AODC measurements, 1 cm^3 of sediment was injected into serum vials containing 9 mL of filter-sterilized seawater that had been pre-amended with formaldehyde (3.8% final concentration v/v; MF-Millipore Membrane Filters, 0.22 μm). Sediment slurries were prepared by vortexing the serum vials for 5 min. Immediately following agitation, triplicate subsamples were stained with acridine orange (final AO concentration 0.01%) for 3 min (Hobbie *et al.*, 1977). At least 100 cells or 100 fields of view were microscopically counted for each slide prepared.

Lipid extractions and derivatization

All glassware and metal tools used for lipid extractions were baked at 460 °C for 8 h. All Teflon-lined caps and stoppers were rinsed with both chloroform and methanol prior to use. Sediment cores were lyophilized, after which

2 mm of sediment was scraped from the outside surface areas and discarded. Depending on depth and AODC cell number estimates, 35–147 g (dry weight) of sediment was extracted for each sample. Each sample was divided among several 200-mL-glass centrifuge tubes to maximize extraction efficiency. Sediments then underwent two total lipid extractions following the modified Bligh–Dyer method (White & Ringelberg, 1998). Total lipid extracts were combined and evaporated under nitrogen. Phospholipids were separated from less polar lipids using solid phase extraction (SPE) cartridges (Alltech part #209200) and derivatized to fatty acid methyl esters (FAMEs) by mild alkaline methanolysis (White & Ringelberg, 1998). Dimethyl disulfide derivatives were produced from selected FAME samples to determine the point of unsaturation within monounsaturated structures (White & Ringelberg, 1998).

Phosphoether lipids (PEL) were separated from FAMEs using the same SPE columns as above and were subjected to hydriodic acid cleavage and $LiAlH_4$ as described by Koga & Morii (2006). Special care was taken to protect the $LiAlH_4$ reduction from water and the atmosphere, including the use of Na_2SO_4 as a drying agent. The reduction was conducted in sealed culture tubes under argon using tetrahydrofuran dispensed from a Pure Solv Solvent Purifier (Innovative Technology Inc., Amesbury, MA, USA).

FAME and PEL identification and quantification

Fatty acid methyl ester samples and PEL hydrocarbons were analyzed using an Agilent 7890A gas chromatograph equipped with a DB-1 MS column (JBW Scientific, 60 m × 0.32 mm internal diameter; 0.25-micrometre-film thickness) and an Agilent 5975C mass spectrometer at the U.S. Geological Survey in Lakewood, CO. FAMEs were identified by comparing their mass spectra and retention times to FAME standards. Quantification of FAME peaks was based on selected ions. Unique quantification ions were chosen for the different FAME classes based on their dominance in the mass spectrum (short chain and branched fatty acids = 74 + 87, monounsaturated fatty acids = 55 + 69, double unsaturated fatty acids = 55 + 67, cyclic fatty acids = 74, and polyunsaturated fatty acids = 79 + 67 + 91; Dodds *et al.*, 2005). The FAME 13:0 was added to all samples as an internal standard. Response factors were calculated to compensate for response variations between different FAME classes and the 13:0 internal standard.

Phosphoether lipids derivatives were analyzed using the same GCMS and column described above. The GC program started with a 2 min hold at 70 °C and then ramped from 70 to 130 °C at 20 °C with 1 min hold, 130 to 190 °C at 4 °C min^{-1} with a 2 min hold, and finally 190 to 250 °C at 4 °C min^{-1} with a 20 min hold.

FAME stable carbon isotope ratios

The $\delta^{13}C$ of the FAMEs were measured using a Delta V plus GC- IRMS interfaced to a Thermo Trace GC with a split/splitless injector on a Restek Rxi-5MS column (60 m × 0.25 mm id, ×1.0-μm-film thickness; Skidaway Institute of Oceanography, Savannah, GA, USA). Isotopic values were corrected for the added carbon during methylation, and final values were reported in the standard δ notation and expressed against VPDB.

DNA extraction, PCR, and sequencing

DNA was extracted from 0.2 g of sediment using the Powersoil extraction kit from MoBio, Inc. (Carlsbad, CA, USA). Universal forward and reverse PCR primers were selected to flank the V4 and part of the V5 hypervariable region of the SSU rRNA gene as described in Baker *et al.* (2003). Forward primers included the 454 life science A adapter, a distinct 8 basepair (bp) barcode, a two bp linker, and the 515F primer (5′-GCCTCCCTCGCGCCATCAG-barcode-CA-GTGCCAGCMGCCGCGGTAA-3′) Primer coverage of Bacterial and Archaeal domains with two mismatches is 80.7% and 65.8%, respectively (Cole *et al.*, 2009). The reverse primer included the 454 life science B sequencing adapter, a two bp linker, and the 926R primer (5′-GCCTTGCCAGCCCGCTCAG-TC-CCGTCAATTCMTTTRAGTTT-3′). Coverage of Bacterial and Archaeal domains with two mismatches were 65.8% and 75.1%, respectively (Cole *et al.*, 2009).

PCRs for the samples were conducted using Promega Master Mix (Madison, WI, USA), and the amplicons were normalized using Invitrogen's SequalPrep Normalization Plate Kit (Carlsbad, CA, USA). The normalized amplicons from each sample were then pooled together, gel purified, and sequenced on a 454 FLX Sequencer at the Denver Health Science Center (Denver, CO, USA).

Phylogenetic analysis

Pyrosequencing reads were analyzed using the QIIME software pipeline (Caporaso *et al.*, 2010a,b). Reads outside 200–300 nucleotides in length, with a minimum quality score lower than 27, or incorrect barcodes were discarded from further analyses. In total, 27 962 pyrosequencing reads among the 15 samples qualified for further processing. Sequences were denoised using the QIIME denoiser and clustered into operational taxonomic units (OTUs) at 97% similarity using the UCLUST furthest neighbor algorithm (Edgar, 2010). OTUs were aligned using PyNAST (Caporaso *et al.*, 2010a,b), and chimeras were identified and removed using QIIME's ChimeraSlayer. Taxonomy was assigned by comparing OTUs against the Silva database using the Basic Local Alignment Search Tool (BLAST; Altschul *et al.*, 1990; Pruesse *et al.*,

2007). Samples were rarefied to 1130 sequences (with the exception of sample 30–35 cmbsf, which only had 421 sequence reads); after which, rarefaction curves, Chao1 estimates and the Shannon Index were created using QIIME software to assess diversity (Shannon & Weaver, 1949; Chao, 1984). Given that QIIME calculates the Shannon Index using $\log_2$ instead of ln, results calculated by QIIME were corrected by multiplying values by ln(2).

Principal component analyses

Changes in PLFA and OTU profiles were analyzed by principal components analysis (PCA). Relative contributions of individual PLFAs and OTUs were used as input values for each PCA. The analyses were conducted using MINITAB 16 statistical software (Minitab Inc., State College, PA, USA). Variables differing from a normal distribution were normalized using a Johnson transformation algorithm (Chou *et al.*, 1998). Loading scores for the individual PLFAs or OTUs were used to assess the influence individual OTUs had on the calculated principal component axes.

RESULTS

Geochemistry

Porewater chemistry shows that these sediments are oxic with no dramatic shifts in redox states or carbon availability to 1.5 cmbsf (Fig. 2). With the exception of one apparent outlier at 135–140 cmbsf, dissolved O_2 concentrations decreased with depth, reaching a minimum of 252 μM at 145–150 cmbsf. Analytical drift for O_2 measurements was not accounted for and may have resulted in possible errors. However, the dissolved O_2 profile is reasonable compared to the other porewater results, which are also consistent with an oxic environment throughout the top 1.53 mbsf. Sulfate concentrations were similar to seawater concentrations fluctuating between 29 and 27 mM. Concentrations of NO_3^-, NO_2^-, and NH_4^+ all show a similar profile with depth. Concentrations of NH_4^+ reached three local maxima at approximately 17, 47, and 87 cmbsf. Increased concentrations of NO_3^- and NO_2^- exist at 37 and 107 cmbsf. Both NO_3^- and NO_2^- are undetectable at 55–60 cmbsf [limits of detection 0.16 and 0.08 μM, respectively (Ball *et al.*, 2008)]. Nitrite is also below detection at sample depths 15–20 and 55–60 cmbsf. Alkalinity and $\delta^{13}C_{DIC}$ remain relatively constant with depth at approximately 3 mM and −3‰, respectively. Similarly, bulk sediment measurements show small changes with depth. POC and $\delta^{13}C$ values were on average 0.18 wt% and −22.7‰, respectively.

Acridine orange direct cell counts

Direct cell counts were highest in the top surface sediments (0–10 cm) with approximately 1.7×10^7 cells mL^{-1} and decreased to 1.3×10^6 cells mL^{-1} down

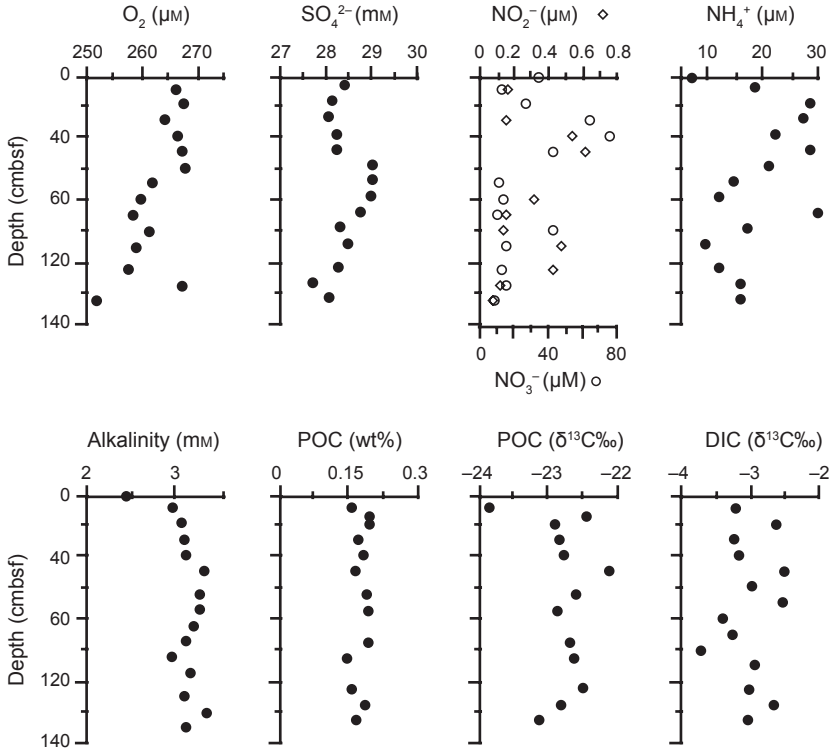

Fig. 2 Porewater geochemistry profiles with depth. Values at 0 cmbsf represent seawater measurements made just above the seafloor.

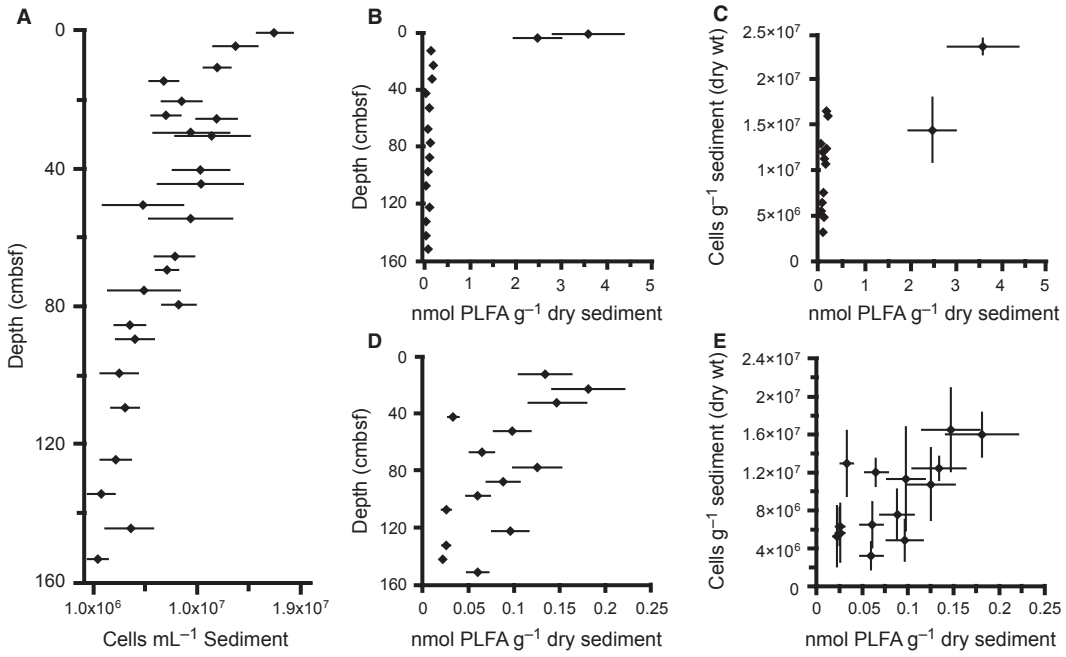

Fig. 3 Estimates and comparisons of cell density with depth by (A) acridine orange direct counts (AODC) and (B) Total phospholipid fatty acid (PLFA) concentrations. (C) Comparison between total PLFA concentrations and AODC cell counts. (D) Total PLFA concentrations for sediment interval 10–153 cmbsf. (E) Comparison between total PLFA concentrations and AODC cell counts for sediment interval 10–153 cmbsf. Cell counts were converted to units of cells g^{-1} sediment (dry weight) using porosity data.

the 153 cm core (Fig. 3A). Standard deviation averaged 33%.

Total phospholipid concentrations

Phospholipid fatty acids and PELs were derivatized and measured as FAMEs and phytane, respectively, to estimate viable cell concentrations. FAME concentrations within the top 0–2 and 2–5 cmbsf were significantly greater than those below, reaching 3.69 and 2.66 nmol g dw^{-1}, respectively (Fig. 3B, Table 1). Concentrations between 10 and 153 cmbsf ranged between 1.34 and 0.22 nmol g dw^{-1} generally decreasing with depth. The total concentration of FAMEs at 40–45 cmbsf is relatively low (0.32 nmol g dw^{-1}) compared to the surrounding samples, and total FAME concentrations reach a minimum at 140 cmbsf. Isoprenoid lipids of archaeal membranes were not detected in any of the samples; however, the Bligh and Dyer extraction and subsequence preparation steps are known for low PEL recoveries (Nishihara & Koga, 1987; Lengger *et al.*, 2012).

FAME compositions

Compositional analysis of FAMEs was used to aid SSU rRNA characterization of the microbial community. The relative molar abundances of individual FAMEs are shown in Table 1. Monounsaturated (MUFA) and short-chain (<c20) fatty acids are the most dominant FAMEs throughout the core, with averages of 28.4 and 48.7 mol%, respectively. Overall, 16:0 (average 29.9%) is the most dominant FAME while 18:0 (13.9%), 16:1ω7 (10.0%), 18:1ω7 (7.23%), and 18:1ω9 (6.1%) are also abundant. Large percentages of MUFA are often associated with Gram-negative bacteria, which were abundant among sequencing results (Phylogeny and diversity, Fig. 5). Lower amounts of long chained (>C20) and methyl-branched chains are present at all depths, with averages of 6.5 and 10.2 mol%, respectively. Interestingly, several diunsaturated fatty acids (DUFA) and polyunsaturated fatty acids (>2 points of unsaturation, PUFA) were found in the surface sediments and between 85 and 105 cmbsf, suggesting the presence of either eucaryotes and/or PUFA-producing bacteria. DUFAs and PUFAs include 18:2, 20:4, 20:5, 20:2, and 22:6.

FAME δ^{13}C values

Phospholipid fatty acids of sufficient quantity were measured for stable carbon isotopes and are presented in Fig. 4 and Table 2. PLFAs measured in triplicate exhibited deviations less than ±0.9‰. While some $\delta^{13}C_{PLFA}$ values fluctuate more than others, they are depleted relative to POC and DIC (Fig. 4) and consistently near −32‰ throughout the core. This suggests that microbial metabolisms change

Table 1 Total and relative PLFA abundances

Depth (cmbsf)	0–2	2–5	10–15	20–25	30–35	40–45	50–55	65–70	75–80	85–90	95–100	105–110	120–125	135–140	145–150	150–153
nmol PLFA g (dw)$^{-1}$	3.58	2.47	0.13	0.18	0.15	0.03	0.10	0.06	0.12	0.09	0.06	0.03	0.10	0.03	0.02	0.06
Mole% of total PLFA																
i14:0	0.5	0.8	0.5	1.1	0.9	0.0	2.1	0.8	0.4	0.3	0.7	0.6	0.3	0.5	0.2	0.5
14:0	2.4	3.6	3.3	4.9	5.3	4.6	2.7	3.5	3.0	2.2	3.7	3.5	2.0	3.9	2.0	5.6
i15:0	2.4	2.7	2.2	3.9	3.2	2.9	2.2	2.2	1.7	1.4	2.6	2.8	1.2	2.7	1.7	1.7
a15:0	2.0	5.2	3.4	5.9	5.8	4.2	2.3	3.3	2.7	1.6	3.3	4.2	1.7	3.8	2.6	2.5
15:0	0.4	1.0	1.0	1.5	1.8	1.9	2.3	1.6	1.3	0.8	1.3	1.7	0.7	1.5	1.3	0.9
11me15:0	0.0	0.5	0.3	0.3	0.6	0.0	0.0	0.3	0.2	0.0	0.2	0.0	0.0	0.3	0.2	0.0
i16:0	0.8	2.0	0.5	0.7	1.0	1.1	0.0	1.2	0.9	0.7	1.1	1.3	0.5	1.0	1.0	0.7
16:1w9	2.4	2.4	2.0	3.5	1.9	0.3	0.0	0.0	0.8	0.8	0.7	0.0	0.3	0.3	0.0	0.0
16:1w7	16.7	13.9	10.7	20.9	14.0	7.7	8.9	7.8	4.7	6.3	5.0	7.1	5.7	12.3	10.7	9.3
16:1*	0.5	0.8	0.7	0.5	0.0	0.0	0.0	0.0	0.0	0.0	0.4	0.0	0.0	0.2	0.0	0.0
16:1w5	5.4	5.2	3.4	6.0	3.1	1.9	0.0	2.2	1.2	1.7	1.2	2.9	0.9	1.4	1.5	1.6
16:0	15.1	14.4	36.0	17.3	17.3	32.4	46.2	37.4	43.7	29.4	34.1	34.9	39.5	28.9	35.0	17.2
i17:0	0.9	0.5	1.8	2.3	4.1	1.6	0.0	1.8	1.4	0.8	1.3	1.7	0.6	1.3	1.8	0.5
8me16:0	0.3	0.7	0.5	0.8	0.7	0.5	0.0	0.6	0.2	0.6	0.6	0.3	0.0	0.6	0.0	0.0
5me16:0	0.7	1.0	0.6	1.1	0.9	0.5	8.8	0.6	0.4	0.5	0.6	0.6	0.0	0.5	0.0	0.0
17:1w8	1.6	2.0	0.0	3.5	0.0	0.0	0.0	0.0	0.0	0.0	4.6	0.0	13.5	0.0	0.0	0.0
cy17:0	1.7	2.1	4.7	0.0	0.0	0.0	0.0	0.0	0.0	0.0	0.0	0.0	0.0	0.0	0.0	0.0
17:0	0.3	0.5	0.5	0.8	0.8	0.5	2.7	0.0	0.7	0.5	0.7	0.9	0.3	0.6	0.9	0.4
18:2	0.9	0.7	0.0	0.0	0.0	0.0	0.0	0.0	0.0	0.0	0.0	0.0	0.0	0.0	0.0	0.0
18:1w9	3.3	3.8	1.9	3.8	22.7	4.0	1.6	1.6	2.5	1.5	1.0	4.0	1.4	3.5	5.6	36.0
18:1w7	16.9	13.1	6.8	15.0	6.0	11.4	1.7	3.9	2.7	6.5	3.3	7.4	2.6	6.2	7.2	5.5
18:0	3.8	5.1	16.0	2.1	2.8	13.9	8.6	22.3	23.9	16.1	16.2	16.6	25.1	23.7	17.1	8.9
cy19:0/19:1*	0.1	1.3	0.0	0.0	0.0	0.0	0.0	0.0	0.0	1.1	0.6	0.0	0.0	0.0	0.0	0.0
cy19	0.2	2.1	0.0	0.0	0.0	0.0	0.0	0.0	0.0	0.0	0.0	0.0	0.0	0.0	0.0	0.0
20:4	8.2	9.9	0.0	0.0	0.0	0.0	0.0	0.0	0.0	21.7	8.6	0.0	0.0	0.0	0.0	0.0
20:5	5.5	2.5	0.0	0.0	0.0	0.0	0.0	0.0	0.0	0.0	3.5	0.0	0.0	0.0	0.0	0.0
20:2	0.8	0.4	0.0	0.0	0.0	0.0	0.0	0.0	0.0	1.6	0.0	0.0	0.0	0.0	0.0	0.0
20:1w9	0.9	1.2	0.0	0.0	0.0	0.0	0.0	0.0	0.0	0.0	0.0	0.0	0.0	0.0	0.0	0.0
20:1w7	0.6	0.7	0.0	0.0	0.0	0.0	0.0	0.0	0.0	0.0	0.0	0.0	0.0	0.0	0.0	0.0
20:0	0.2	0.2	0.5	0.7	1.4	1.9	0.0	1.7	1.4	0.8	0.9	1.9	0.0	1.5	2.1	5.4
22:6	2.7	0.0	0.0	0.0	0.0	0.0	0.0	0.0	0.0	0.0	0.0	0.0	0.0	0.0	0.0	0.0
22:0	0.5	0.6	1.0	1.4	2.5	3.8	0.0	3.0	2.5	1.4	1.7	3.4	1.9	2.5	3.7	1.7
23:0	0.1	0.1	0.3	0.0	0.0	0.0	0.0	0.0	0.7	0.3	0.4	0.0	0.0	0.0	1.1	0.0
24:0	0.9	0.7	1.0	2.0	3.1	4.9	9.9	4.2	2.9	1.6	1.8	4.2	1.9	2.8	4.3	1.8
Total SCFA	21.9	24.6	56.8	26.6	27.9	53.3	62.4	64.9	72.6	48.9	55.9	57.7	67.7	58.7	56.3	32.9
Total LCFA	1.6	1.6	2.9	4.0	7.0	10.7	9.9	8.9	7.6	4.2	4.9	9.4	3.8	6.8	11.2	8.9
Total BRFA	8.1	13.6	9.6	16.2	17.2	10.7	15.5	10.8	8.0	5.8	10.3	11.5	4.2	10.6	7.5	5.9
Total MUFA	48.4	43.0	25.5	53.1	47.6	25.4	12.2	15.5	11.8	16.7	16.3	21.4	24.3	23.9	25.0	52.3
Total DUFA	1.7	1.2	0.0	0.0	0.0	0.0	0.0	0.0	0.0	1.6	0.0	0.0	0.0	0.0	0.0	0.0
Total PUFA	16.5	12.4	0.0	0.0	0.0	0.0	0.0	0.0	0.0	21.7	12.0	0.0	0.0	0.0	0.0	0.0
Total CyFA	1.9	5.5	4.7	0.0	0.0	0.0	0.0	0.0	0.0	1.1	0.6	0.0	0.0	0.0	0.0	0.0

SCFA, short chain fatty acid (>20 carbons); LCFA, long chain fatty acid (>20 carbons); BRFA, branched fatty acids; CyFA, cyclic fatty acids; DUFA, diunsaturatred fatty acids; MUFA, monounsaturated fatty acids; PLFA, phospholipid fatty acids; PUFA, polyunsaturated fatty acids. *Point of unsaturation not determined.

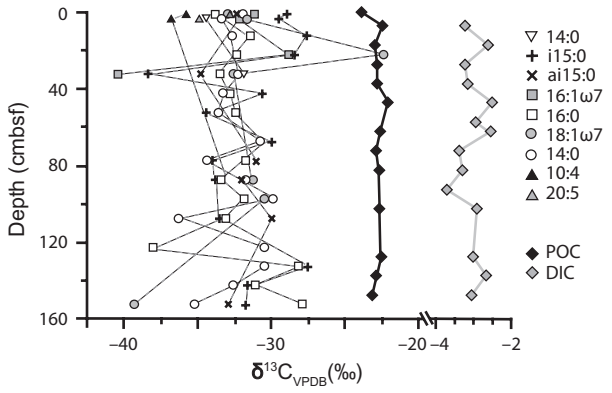

Fig. 4 $\delta^{13}C$ values of phospholipid fatty acids (PLFAs) and possible carbon sources with depth (cmbsf).

little within these sediments. Iso15:0 and 16:1ω7 have heavier $\delta^{13}C$ values in the top 20 cm (approximately −28‰), but show a 10‰ depletion at 32.5 cmbsf, representing the lightest PLFAs detected in these sediments. 16:0 also shows a approximately 10‰ change over a single depth interval, shifting from −37‰ at 120 cmbsf to −28‰ at 130 cmbsf.

Phylogeny and diversity

The SSU rRNA gene was sequenced from genomic DNA extracted from 15 depths throughout the core to measure diversity and elucidate metabolic pathways. Fifty bacterial phyla were identified by the SSU rRNA sequences. The most dominant phyla included Actinobacteria, Bacteroidetes, Chloroflexi, Firmicutes, and the subphyla β-, δ-, and γ-Proteobacteria (Fig. 5). Other phyla that represent at least 1% of the bacterial population at one or more sample depths include Acidobacteria, Candidate Division OP3, Candidate Division OP9, Cyanobacteria, Deferribacteres, Deinococcus-Thermus, Planctomycetes, and α-Proteobacteria.

Chloroflexi, Firmicutes, Actinobacteria and Bacteroidetes

On average, Chloroflexi make up 25% of the sequenced community and are most abundant at 50–55 cmbsf, making up 61% of OTUs. Of the 289 Chloroflexi OTUs sequenced, 52% of Chloroflexi sequences were assigned to the uncultured subphylum lineage VadinBA26 (vinesses anaerobic digester of Narbonne) while classes Anaerolinaea and Caldilineae of subphylum I each represented 11% of Chloroflexi sequences. Actinobacteria are found relatively evenly throughout the core at approximately 6%, with the exception of 150–153 cmbsf, where they were absent. Abundances of Firmicutes fluctuated through the core, reaching more than 14% at 85–90 and 130–140 cmbsf. Within the phylum Firmicutes, 98% of sequenced OTUs fall into the classes of Bacilli and Clostridia. Bacteroidetes are most abundant in the deepest sediment, making up 46% of the sequenced population at that depth.

Proteobacteria

Betaproteobacteria OTUs were found in high abundances (>20%) at depths 30–35, 40–45, 65–70, 75–80, and 150–153 cmbsf. At these depths, over 45% of β-Proteobacteria OTUs were classified as the Family Hydrogenophilacaea and more specifically, the genera *Thiobacillus* and *Teptidiphius*. Gammaproteobacteria on average represented 8% of OTUs at all sample depths except 120–125 cmbsf, where they represent 40% of sequences. OTUs of γ-Proteobacteria were primarily classified as Pseudomonads, Xanthomonadaceae, and Enterobacteriales. Small percentages (approximately 2–3% of total γ-Proteobacteria) of Shewa-

Table 2 $\delta^{13}C$ values (‰) for phospholipid fatty acids (PLFAs)

	PLFA									
Depth cmbsf	13:0	14:0	i15:0	ai15:0	16:1ω7	16:0	18:1ω7	18:0	20:4	20:5
0–2	−34.6	−32.9	−28.9	−32.3	−31.1	−33.8	−32.9	−31.9	−35.8	−32.8
2–5	−33.8	−34.5	−29.5	−32.2	−32.2	−33.3	−31.6	−33.4	−36.8	−34.9
10–15	−34.0		−27.6			−31.4		−32.7		
20–25	−34.3		−28.5		−28.8	−32.3	−22.4			
30–35	−34.7	−31.8	−38.4	−34.8	−40.5	−33.5	−32.6	−32.3		
40–45	−30.8		−30.6			−32.8		−33.3		
50–55	−33.0		−34.4			−32.4		−33.6		
65–70	−33.5		−30.0			−30.6		−30.7		
75–80	−34.4		−34.0	−31.0		−31.7		−34.4		
85–90	−34.8		−33.8	−32.0		−33.4	−31.3	−31.7	−33.0	
95–100						−31.8	−30.4	−29.9		
105–110	−31.6		−33.5	−29.9		−33.1		−36.3		
120–123	−32.2					−38.0		−30.4		
130–135	−31.9		−27.5			−28.1		−30.4		
140–145	−34.1		−31.6			−31.1		−32.6		
150–153	−34.2		−31.8	−33.0		−27.9	−39.3	−35.2		

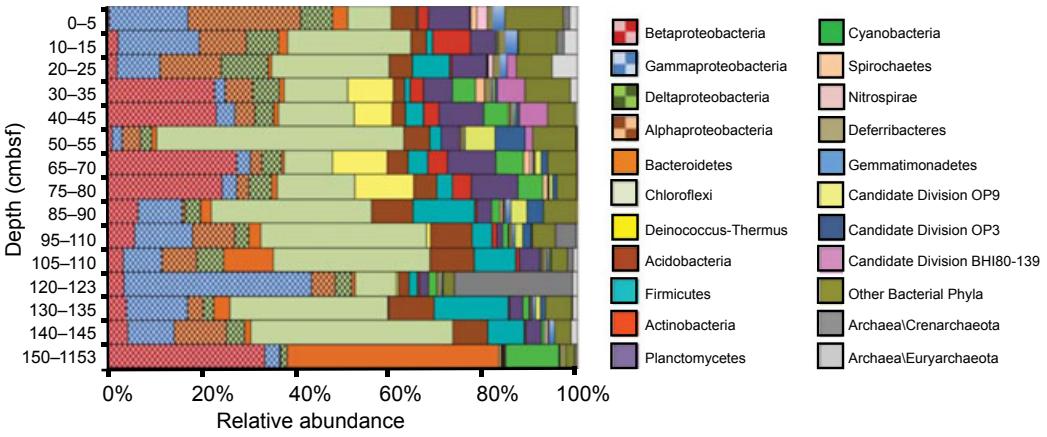

Fig. 5 Relative phylogenic abundances at the phylum and subphylum level as determined by SSU rRNA gene sequencing. The bacterial and archaeal groups shown here represent at least 1% of the sequenced community at any given depth.

nellaceae were present at 40–45, 85–90, and 95–100 cmbsf. Deltaproteobacteria represent 25% of the sequenced community at 0–2 cmbsf and an average of 7% throughout the rest of the core, except for sediments at 85–90 and 150–153 cmbsf, where they represent <1% of OTUs.

Archaea

Archaea sequences were found to represent <4% of OTUs, which is comparable to other methane-free marine settings (Vetriani *et al.*, 1999; Bowman *et al.*, 2003). Euryarchaeota represent on average 1% of the sequenced community and as much as 5% of OTUs at 20–25 cmbsf. At 120–125 cmbsf, members of the Crenarchaeota make up 25% of OTUs, with 93% of sequences grouping into the Miscellaneous Crenarchaeotal Group (MCG). This relatively high percentage of Crenarchaeota is unexpected given no detectable isoprenoids in the sediments and raises questions whether the extracted DNA translates to active and viable cells.

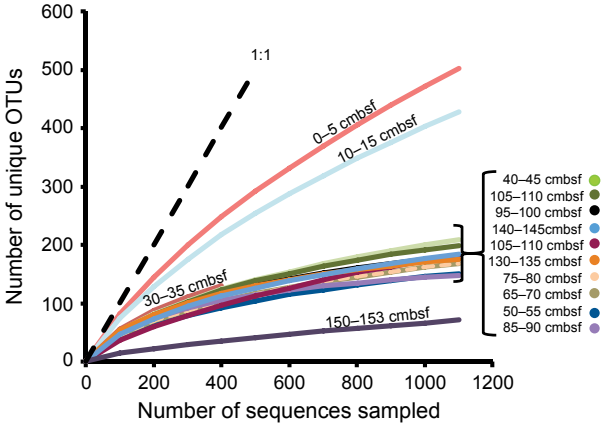

Fig. 6 Rarefaction curves for all samples, a few distinct samples are labeled by depth (cmbsf). Plots illustrate that sediments at 0–15 cmbsf harbor more unique operational taxonomic units (OTUs) than those collected at 20–152 cmbsf.

Diversity

Rarefaction curves were generated for each depth to evaluate the thoroughness of the SSU rRNA sequencing (Fig. 6). Rarefaction plots compare the number of unique OTUs identified to the number of sequences subsampled. Thorough sampling efforts are achieved when the number of unique OTUs approaches a limit described by the upper bound of the rarefaction curve. Incomplete sampling would continue to follow a slope of 1. Rarefaction curves generated using sequences sampled from 20 to 153 cmbsf all approach an upper bound. Rarefaction curves for the shallowest sediments illustrate that additional sampling would reveal more unique OTUs and increase diversity. This observation is also mirrored by the Chao1 species richness (Fig. 7), which estimates the number of unique OTUs in a sample based on the number of OTUs that are represented by only one or two sequences (Chao, 1984). Chao1 estimates are as high as 1166 (±7.6%) in surface sediments and drop to an average of 284.7 (±34.3%) OTUs below 20 cmbsf and show no apparent trend with depth.

Because biodiversity is not only a measure of species abundance but also species distribution, the Shannon Index, a measure of both richness and evenness, was calculated (Fig. 7; Shannon & Weaver, 1949). The Shannon Index ranges from high to low, where 0 represents a single organism community and 7 represents the theoretical maximum of richness and evenness, where all 1130 sequences represent a unique OTU. Here, the largest Shannon Index value calculated (5.7) was derived from the top five centimeters of sediment. The lowest values (3.1 and 2.1) were calculated for samples 120–125 and 150–153 cmbsf.

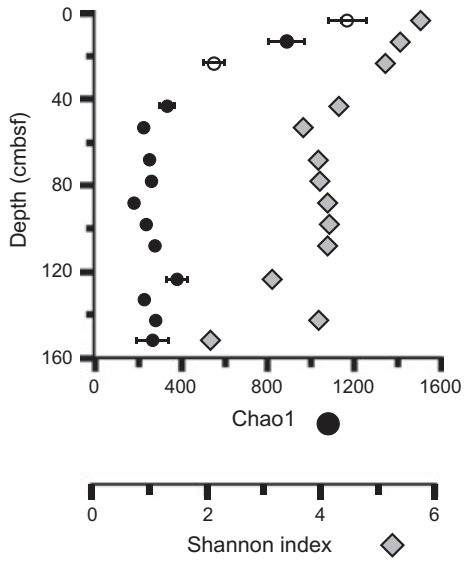

Fig. 7 Depth profiles Chao1 (black ●) and the Shannon Index (gray ◆), demonstrating diversity based on estimated richness and evenness respectfully. In both cases, diversity decreases with depth.

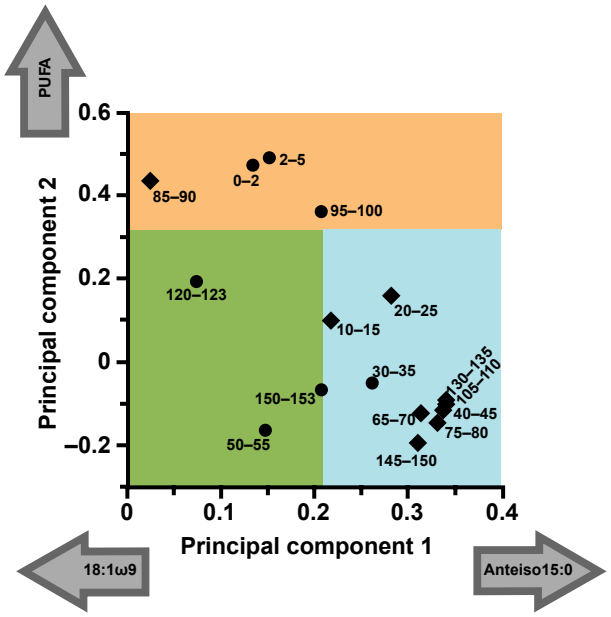

Fig. 8 Principal component analysis of measured phospholipid fatty acids (PLFAs) detected at all sample depths, excluding the most abundant PLFAs that are generally considered ubiquitous among microbial species (e.g., 16:0, 16:1ω7, 18:0, and 18:1ω7).

Principal component analysis

Principle component analysis of PLFA and OTU profiles were performed to identify similarities among samples. When PCA was conducted on PLFA profiles, the first principal component explained 83% of the variance and, according to loading scores, was controlled by relative abundances of the most dominant PLFAs: 16:0, 16:1ω7, 18:0, and 18:1 ω7. These fatty acids are known to be ubiquitous throughout the bacterial domain and do not lend much insight into the microbial community structure. Further PCA that excluded these major lipids is presented in Fig. 8. Principal Component 1 and 2 account for 50% and 15% of the variance, respectively, and PLFAs with relatively large loading scores include 18:1w9, 14:0, anteiso15:0 and 20:4. Samples with relatively large amounts of anteiso15:0 plot above 0.2 along PC1 and may represent the presence of Gram-positive bacteria. Similarly, samples containing PUFA plot above 0.3 along PC 2 and represent a PUFA-producing source.

The first two PCs calculated from PCA performed on sequenced OTUs account for 33% and 19% of the total variance (Fig. 9). Samples plotted into three groups, all of which had positive PC1 values. The samples of group I had PC 1 values below 0.15 and included shallow sediments 0–25, 120–125, and 105–153 cmbsf. Group II had PC 1 values larger than 0.15, negative PC 2 values and included 30–25, 40–45, 65–70, and 75–80 cmbsf. Group III had PC 1 values >0.15, positive PC 2 values, and included all remaining samples. According to the loading scores OTUs belonging to the phyla Chloroflexi have a positive influence on PC1 and PC 2, while Deinococcus-Thermus and Betaproteobacteria had a positive effect on PC1 but a negative effect on PC2.

DISCUSSION

Biodensity estimates and relevance to global microbial distributions

The ANDRILL Program provided a rare opportunity to sample deep-sea sediments from beneath a permanent ice shelf for microbiological studies. Although the overall distribution of bacteria in deep-sea sediments is controlled by several important environmental factors, in general, there is a global logarithmic decline in microbial populations with increasing sediment depth (Parkes *et al.*, 2000). This was also evident at the ANDRILL site where cell numbers decrease by one order of magnitude over the top 150 cm of sediment. Microbial estimates derived from AODC of the surface sediments at the ANDRILL site were 1.7×10^7 cells mL^{-1}. These cell densities are considerably lower than those reported for most near-shore, shallow sediments (approximately 10^8 cell mL^{-1}; Fig. 10A, Table S1), but 100× greater than deep-sea, open ocean sites such as the South Pacific Gyre (water depth > 4000 m, cell densities approximately 10^5 cells mL^{-1}; D'Hondt *et al.*, 2009; Expedition 329 Scientists, 2011). Our reported densities agree well with those from the deep-sea sediments of the Peru Margin (ODP site 1225, 2°46.25′N, 110°34.29′W), which range from approximately 10^7 cells mL^{-1} near the

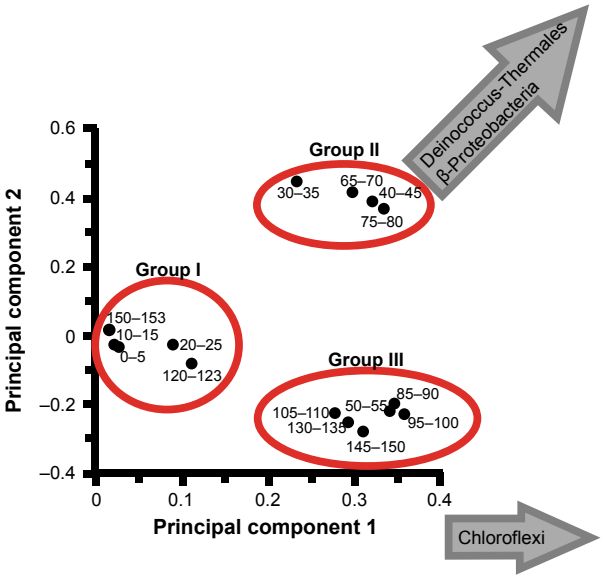

Fig. 9 Principal component analysis of sequenced operational taxonomic units (OTUs) identified from sediments collected between 0 and 153 cmbsf.

surface and drop to approximately 7.5×10^6 cells mL^{-1} at approximately 85 cmbsf (D'Hondt *et al.*, 2003). Unlike most continental settings, sea ice limits primary productivity and restricts OC inputs to the sediments. Therefore, the relatively low cell numbers observed in surface sediments of the Ross Sea seem reasonable.

The overall abundance of bacteria, spatially, in deep-sea sediments will ultimately depend on the availability of suitable nutrients and energy sources. A positive correlation is observed between population size and sedimentation rate, a proxy for OM flux, as shown in Fig. 10A. This figure was generated from the shallowest cell abundance estimates (<10 mbsf) of various near-shore and deep ocean environments (see Table S1 for references). Hypothesis testing strongly suggests the observed linear regression to be significant (P-value < 0.005, $R^2 = 0.4$), illustrating that shallow sites with higher sedimentation rates generally have higher microbial densities. Alternatively, lower microbial abundances of deep-sea sediments not only reflect decreased OM input, but also increased exposure and degradation of OM within the water column (Deming *et al.*, 1992). A similar correlation between sedimentation rates and microbial biomass was also recently documented by Kallmeyer *et al.* (2012), as well as others who used ocean photosynthetic productivity as a proxy for OM flux (Deming *et al.*, 1992; Lochte, 1992; Franco *et al.*, 2007; Jørgensen & Boetius, 2007; D'Hondt *et al.*, 2009).

Although sedimentation rates appear to be a good proxy for reactive carbon, phytodetritus is not the only source of reactive carbon in marine settings. In a review of marine aquatic systems, correlation studies indicate that only 32% of bacterial production results from phytoplankton carbon sources (Fouilland & Mostajir, 2010). Additional sources of carbon include allochthonous terrestrial sources and viral cell lysis. Viral mortality has also been credited as a major source of labile carbon in subsurface environments (Danovaro *et al.*, 2008; Jiao *et al.*, 2010). Within the analyses of this study, it is not possible to trace the dominant sources of OM at this site; however, phytodetritus, terrestrial weathering, and viral mortality may all contribute to the labile carbon pool.

There appears to be no trend between sediment POC (wt%) and microbial abundance (Fig. 10B). This observation suggests that not all POC, which includes refractory humic compounds, is available for microbial assimilation and that refractory carbon may be stored in sediments for long periods of time. Ultimately, it appears that the flux of fresh OC has the greatest influence on viable microbial abundance.

Bacterial abundances based on PLFA concentrations

To obtain cell number estimates from phospholipid analyses, a conversion factor that relates measured phospholipids to direct cell counts is required (Haack *et al.*, 1994). Conversion factors based on culture studies range from 2×10^7 to 5.9×10^7 cells nmol $PLFA^{-1}$ (Green & Scow, 2000). Such estimates generally assume that all microbial cells contain 100 μmol PLFAs g^{-1} (dry weight) (White *et al.*, 1979); however, studies have shown that taxonomic differences as well as growth conditions can affect the concentration of phospholipids per cell (Haack *et al.*, 1994; Summit *et al.*, 2000). For example, some cultured species of the phyla Firmicutes and Bacteroidetes generate reduced amounts of phospholipids, as low as 11.4 and 42.3 μmol PLFA g^{-1} (dry weight), respectively (Haack *et al.*, 1994). These two phyla are often present in marine sediments, each representing approximately 5% of the sequenced communities at this site, and may be one reason why past efforts to validate PLFA conversion factors generally produce cell numbers that are less than AODC estimates (Ludvigsen *et al.*, 1999; Summit *et al.*, 2000; Jiang *et al.*, 2007). This is understandable given that PLFA estimates are believed to target only living cells (Harvey *et al.*, 1986) whereas AODC might also include non-viable cells (Smith & D'Hondt, 2006).

To further assess the reliability of published PLFA-based conversion factors, cell numbers were calculated from our measured PLFA concentrations using a conversion factor of 5.9×10^7 cells nmol $PLFA^{-1}$ (Mills *et al.*, 2006; Rütters *et al.*, 2002; Fig. 3C,D). The selection of a larger conversion factor was made based on the comparative studies of Rütters *et al.* (2002) and Summit *et al.* (2000) which used the conversion factors 5.9×10^7 and 2.5×10^7 cells nmol $PLFA^{-1}$, respectively. Both studies

compared AODC to PLFA-based cell densities; however, results were more comparable when the larger conversion factor was utilized (Mills *et al.*, 2006). Given that microbes of the subsurface are suspected to be smaller than those grown in culture (Kallmeyer *et al.*, 2012), it is logical to assume that a given quantity of PLFAs would equate to a higher number of cells.

At this site, PLFA-based estimates are greater than AODC by an order of magnitude in the shallow sediments. Below 5 cmbsf, PLFA-based estimates are usually lower than AODC, but comparable within a factor of 2.5. Higher counts by AODC might be caused by fluorescence of mineral grains, staining of inactive cells, or the false assumption that all microbial cells contain the same amount of PLFAs (White *et al.*, 1979; Smith & D'Hondt, 2006; Morono *et al.*, 2009). Possible sources for the additional phospholipids measured in the uppermost sediments include active apochlorotic diatoms (Blackburn *et al.*, 2009), and meiofauna such as nematodes or oligochaetes. PLFA biomarkers of such eucaryotic organisms are known to include PUFAs such as 18:2, 20:5, 20:4, and 22:6 (Dunstan *et al.*, 1993b; Gibson *et al.*, 1995; Jagdale & Gordon, 1997; Volkman *et al.*, 1998), all of which were identified within the top 5 cmbsf of this core. Regardless of PLFA sources, a Spearman's rank correlation indicates a positive trend of higher PLFA concentrations with increasing cell counts, suggesting that both methods provide comparable cell densities. Correlation coefficients of this comparison are 0.53 when all depths are considered or 0.62 when the top five centimeters are excluded (Fig. 3D). Based on this result, the PUFA structures noted above, and the fact that the direct cell counts primarily targeted procaryotic cells, it appears that the top five centimeters of sediment contains increased populations of eucaryotic cells.

Archaeal abundances based on PEL concentrations

The absence of archaeal lipids is surprising considering the presence of archaeal DNA in the sediment. Hydriodic acid cleavage of a 4Me16:0 diether phosphocholine standard (#999984; Avanti Polar Lipids, Inc., Alabaster, AL, USA) did produce phytane with an average recovery of 89.4% ($n = 3$), suggesting that cleavage of the either bond was successful. Loss of PELs is more likely to have occurred during the extraction or separation steps. The Bligh and Dyer extraction protocol is known for low PEL recoveries (Nishihara & Koga, 1987). PEL efficiencies can be improved by replacing the aqueous phosphate buffer with either 2 M HCl or 5% trichloroacetic acid (Nishihara & Koga, 1987); however, this substitution was not made for this study. Recent studies have also shown that preparation steps involving SiO_2 columns and drying agents such as Na_2SO_4 reduce PEL recovery by as much as 80% (Lengger *et al.*, 2012), and therefore PEL analyses were considered inconclusive.

PUFA sources

As noted previously, the top five centimeters of sediment contains increased eucaryotic cells, and likely explains the high concentration of PUFAs. Although eucaryotes may also be the source of PUFAs detected at 85–100 cmbsf, it seems unlikely, given that microeucaryotes often produce multiple PUFAs of varying chain length (Tornabene *et al.*, 1974; Dunstan *et al.*, 1993a,b). Below 5 cm, we only observed PUFAs of 20 carbon length, which is more suggestive of a bacterial source (Freese *et al.*, 2009). The PCA plots based on PLFA and OTU profiles further support alternative PUFA sources for the deeper sediments. While PUFA containing samples cluster together according to PLFA data (Fig. 8), they cluster separately according to SSU rRNA sequences (Fig. 9), suggesting that the organisms responsible for the PUFAs may be different.

To date, known PUFA-producing bacteria include the genera *Flexibacter and Psychroflexus* of the phylum Bacteroidetes and the genera *Shewanella, Colwellia, Halomonas, Phychromonas, Alteromonas, Photobacterium, and Moritella* of the subphylum γ-Proteobacteria. While capable of growth over a range of temperatures, many of these organisms are thought to be psychrophilic or psychrotolerant, utilizing PUFAs to maintain cellular membrane fluidity in cold environments (Delong & Yayanos, 1986; Hazel, 1995; Allen *et al.*, 1999). Temperature appears to have the greatest influence on PUFA production. Studies of pure cultures show that PUFA production increases dramatically when growth conditions are below 20 °C (Nichols *et al.*, 1997; Freese *et al.*, 2009). Temperatures at the water-sediment interface of the deep oceans are universally cold and recorded to be −1.68 °C at the ANDRILL site (Morin *et al.*, 2010), a habitat suitable for PUFA production.

While the short reads of pyrosequencing do not allow taxonomic assignment to the species level, OTUs from the family Shewanellaceae and Colwelliaceaea were sequenced from 10–15, 20–25, 40–45, 65–70, 85–90, 95–100 cmbsf reaching 0.2%, 0.7%, 3%, 1.0%, 3%, and 2% of total OTUs, respectively. Because sequencing results identify DNA from both active and dormant cells, the presence of OTUs do not necessarily indicate viable micro-organisms, or quantitative representations. However, the largest percentages of these OTUs are found at the same depths where PUFAs are most abundant (85–90 and 95–100 cmbsf, Table 1), further supporting the existence of active PUFA-producing bacteria in these deeper sediments.

If psychrophilic bacteria such as Shewanellaceae are responsible for the PUFAs between 85 and 100 cmbsf, then PUFAs would also be expected at 40–45 cmbsf where Shewanellaceae are relatively high compared to other

depths. However, total phospholipid concentrations at 40–45 cmbsf are abnormally low compared to the surrounding depths, perhaps making the PUFAs undetectable.

Richness and evenness

Small subunit rRNA sequencing shows a complex microbial community within these sediments, with thousands of individual OTUs representing 52 bacterial and archaeal phyla. Rarefaction curves, richness and evenness estimators were calculated from sequence data in an effort to observe possible changes in microbial diversity throughout the core (Figs 6 and 7). The top sediments appear to be the most diverse as indicated by high values from the richness and evenness estimators. This increased diversity most likely results from the integration of seawater microbial communities into the sediments and/or more favorable OM quality near the surface. Aside from measuring total POC concentrations, detailed analyses of the DOC fraction were not made. However, it is reasonable to assume that surface sediments hold greater amounts of labile amino acids, fatty acids, and carbohydrates relative to deeper sediments (Wakeham *et al.*, 1997; Keil, 2000) due to continual deposition of phytodetritus. Similarly, increased richness of arctic oligotrophic environments has been positively correlated to phytodetritus inputs, suggesting that increased energy sources support a larger variety of micro-organisms (Bienhold *et al.*, 2012).

Limited OC availability, as suggested by the presence of Actinobacteria and Bacteroidetes, may also be the cause for lower diversity values in the deeper sediments. Relative abundances of Acidobacteria at the ANDRILL site are highest in the deeper sediments, reaching 10% of the total community at 132.5 cmbsf. Acidobacteria are known to be well adapted to oligotrophic conditions (Fierer *et al.*, 2007) and their relative abundance in sedimentary environments has been inversely related to phytodetritus concentrations (Bienhold *et al.*, 2012). Bacteroidetes dominate the microbial community at 150–153 cmbsf. Cultivable strains are known to have hydrolytic and fermentative abilities capable of breaking down complex OC, including cellulose, chitin, and proteins (Cottrell & Kirchman, 2000; Julies *et al.*, 2010). These hydrolytic and fermenting capabilities may give Bacteroidetes an advantage when labile carbon sources become limited (Canfield, 1994).

Principal component analysis of PLFA and OTU profiles

Individual PLFAs were subjected to PCA in an attempt to elucidate covariation patterns among sample depths. PCA resulted in grouped samples according to their relative abundances of Gram-positive bacteria, Gram-negative bacteria, and PUFA-producing organisms (Fig. 8). Loading scores of individual PLFAs indicated that the first PC is positively influenced by increasing concentrations of 14:0 and anteiso15:0, and negatively influenced by 18:1ω9. Fatty acids 14:0, anteiso15:0 and 18:1ω9 are common among many bacteria types; however, it is generally accepted that branched PLFAs represent Gram-positive bacteria, while MUFAs, such as 18:1ω9, represent Gram-negative bacteria (D'Hondt *et al.*, 2002; Mills *et al.*, 2008; Goffredi & Orphan, 2010). Known Gram-positive bacteria sequenced from this site included Actinobacteria and Firmicutes. On average, the sum of these two phyla represents 7.4% of all OTUs (ranging from 0.4% to 16.6%). In general, sample depths with above average abundances of these Gram-positive bacteria (Fig. 8) have higher PC1 values and larger percentages of anteiso15:0. Similarly, samples with relatively large abundances of OTUs belonging to the genus *Meiothermus* have higher PC1 values than

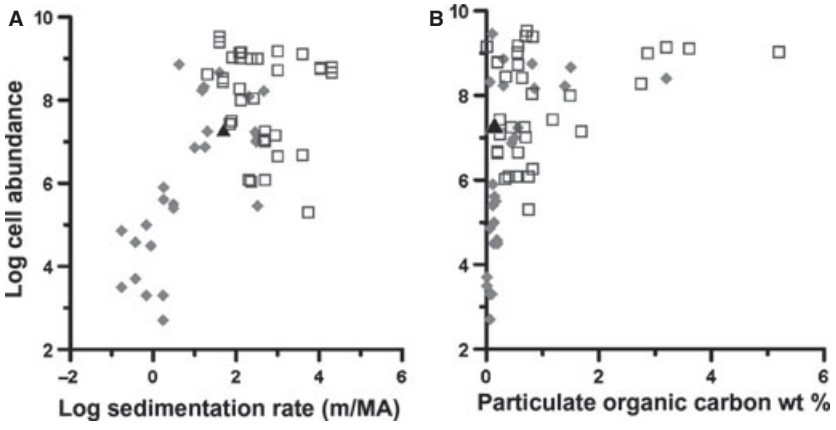

Fig. 10 Cell abundances of marine sediments in relation to sedimentation rates (A) and concentrations of particulate organic carbon (B). Data points represent cell abundances reported for discrete depths of top sediments (<10 mbsf). Sites are grouped by location (□ continental shelves and slopes, ◆ open ocean, ▲ this study; see Table S1 for references).

most samples. While classified as Gram-negative, species of *Meiothermus* have higher abundances of branched PLFAs, including *anteiso*15:0, relative to MUFAs (Cottrell & Kirchman, 2000; Julies *et al.*, 2010).

In contrast, samples 50–55 and 150–153 cmbsf have lower PC1 scores, a relatively larger percentage of 18:1ω9 and relatively large percentages of OTUs belonging to Gram-negative Chloroflexi and Bacteroidetes (Figs 5 and 8). Sample 120–125 cmbsf also has a low PC1 score and contains high proportions of monounsaturated 17:1ω8 (13%) and large proportions of Gram-negative gammaproteobacteria. Similar to 18:1ω9, 17:1ω8 has been attributed to Gram-negative bacteria (Åkerblom *et al.*, 2007), but more specifically, may have originated from gammaproteobacteria in these sediments. Surface samples and sediments collected between 85 and 100 cmbsf have PC2 site scores above 0.3. According to loading scores, PUFA 20:4 is responsible for much of the variation along this axis, suggesting the presence of PUFA-producing bacteria at these sample depths, as discussed above (PUFA sources).

Principal component analysis of sequenced OTUs grouped samples into three distinct groups. According to loading scores, increasing relative abundances of uncultured Chloroflexi belonging to the classes Caldilineae and VadinBA26 have a positive effect on PC1 and separate group I from II and III. Information regarding VadinBA26 organisms is very limited, although studies of cultured Caldilineae indicate the ability to grow heterotrophically and aerobically (Yoon *et al.*, 2010). Based on the observed geochemistry at this site, it is unclear why some samples have larger proportions of these Chloroflexi compared to others. Increasing relative abundance of OTUs belonging to genus Meiothermus, of the phylum Deinoccus-Thermus, and the genus Thiobacillus, of the phylum Betaproteobacteria, were shown to have a positive affect on PC2. Organisms belonging to the genus Meiothermus are generally found in warmer environments (approximately 50–60 °C), so their large presence in these sediments is unexpected (Nobre *et al.*, 1996; Albuquerque *et al.*, 2009). However, both Thiobacillus and Meiothermus are capable of denitrification (Nobre *et al.*, 1996; Miroshnichenko *et al.*, 2003; Beller *et al.*, 2006) and may be responsible for the decline of nitrate and nitrite at 55–60 cmbsf.

Metabolic pathways

Carbon isotope fractionation effects associated with various microbial carbon assimilation pathways ultimately produce $\delta^{13}C_{PLFA}$ values that reflect both the metabolic pathways and carbon sources (Hayes, 2001). However, depending on the $\delta^{13}C$ values of the substrates utilized for a given metabolism, the $\delta^{13}C$ value of cellular biomass cannot always be used as a single indicator to discern the metabolic pathway. For any environment, there can be overlapping ranges of $\delta^{13}C_{biomass}$ values that result from autotrophy and heterotrophy (Mills *et al.*, 2010). Furthermore, isotopic fractionation of assimilated carbon can also occur during lipid synthesis, often resulting in membrane-derived PLFAs that are depleted in ^{13}C relative to the total biomass by as much as −15‰ (Zhang *et al.*, 2003). Despite these variables, $\delta^{13}C_{PLFA}$ values, when referenced to the $\delta^{13}C$ values of available carbon sources (e.g., $\Delta^{13}C_{PLFAs\text{-}DIC}$ and $\Delta^{13}C_{PLFAs\text{-}POC}$), can sometimes indicate metabolisms prevalent within the microbial community (Mills *et al.*, 2006; Oakes *et al.*, 2010). Additional SSU rRNA sequencing can also provide clues to possible metabolisms, and further assist with interpretation of $\delta^{13}C_{PLFA}$ values.

When considering autotrophs and assuming DIC as the sole carbon source, we observed $\Delta^{13}C_{PLFAs\text{-}DIC}$ values ranging from −19.3‰ to −37.4‰ (mean −29.3‰), with the 16:1ω7 having the most depleted $\Delta^{13}C_{PLFAs\text{-}DIC}$ value. According to pure culture studies, of the known autotrophic pathways, only the Calvin–Benson cycle and the acetyl-coA pathway, with fractionation affects of approximately −20‰ and −3% to −36‰, respectively (Preuss *et al.*, 1989; House *et al.*, 2003; Londry & Des Marais, 2003), can explain some of these highly negative $\Delta^{13}C_{PLFAs\text{-}DIC}$ values.

Autotrophic organisms sequenced from theses samples include sulfate-reducing bacteria (SRB), which are capable of metabolizing many organic substrates, but utilize the acetyl-coA pathway for autotrophic or mixotrophic growth (Gibson, 1990). SRB make up 15% of the total sequenced community between 0 and 5 cmbsf, below which they average 2%. Sequenced *Thiobacillus*, which are also abundant in these sediments, are known to grow mixotrophically or autotrophically via the Calvin–Bensen cycle (Coffin *et al.*, 1990; Teece *et al.*, 1999; Zhang *et al.*, 2003). Therefore, the autotrophs identified in these sediments can also grow as mixotrophs and may have $\delta^{13}C_{PLFA}$ values that reflect heterotrophy instead.

The $\Delta^{13}C_{PLFAs\text{-}POC}$ values ranged from +0.4‰ to −17.7‰ (mean −9.2‰), falling within the expected range of 0.3‰ and −7‰ for heterotrophic metabolism (Coffin *et al.*, 1990; Teece *et al.*, 1999; Zhang *et al.*, 2003). Furthermore, the PUFA c20:4 found at 85–90 cmbsf, had a $\Delta^{13}C_{PLFAs\text{-}POC}$ value of −10.3‰, which is consistent with heterotrophy from a PUFA-producing Shewanellaceae. Even the relatively large $\Delta^{13}C_{PLFAs\text{-}POC}$ values of *iso*15:0 (−12.0‰) and 16:1ω7 (−17.7‰) found at 30–35 cmbsf, and of 18:1ω7 (−16.6‰) at 150–153 cmbsf, can result from heterotrophic metabolism if enzymes other than pyruvate dehydrogenase are utilized for acetyl-CoA production. For example, organisms utilizing the enzymes pyruvate formate lyase or acetate kinase with phosphate acetyl transferase can have $\varepsilon_{lipids-biomass}$ values as great as −10.3‰ and −9.4‰, respectively (Teece *et al.*, 1999;

Zhang *et al.*, 2003). Alternatively, the heterotrophs of these sediments may be consuming a ^{13}C-depleted fraction of OM, such as fatty acids, that is not well represented by the average $^{13}C_{POC}$ value (Bickert, 2000). This scenario would be consistent with cell densities and diversity not being correlated with POC concentrations, as observed.

Sequences belonging to heterotrophic organisms represent the majority of sequenced OTUs and include, but are not limited to, the phyla β-, δ-, and γ-Proteobacteria, Actinobacteria, Chloroflexi, and Bacteroidetes. For example, cultivated species of *Caldilinea* and *Anaerolinaea* from the phylum Chloroflexi are known heterotrophic organisms, capable of metabolizing both carbohydrates and peptides (Yamada *et al.*, 2006; Yamada & Sekiguchi, 2009). Bacteroidetes, which were primarily found at 150–153 cmbsf are dominant marine heterotrophs, normally found in organic rich environments (D'Hondt *et al.*, 2002; Mills *et al.*, 2008; Goffredi & Orphan, 2010). Likewise, members of Actinobacteria, Firmicutes, δ-, and γ-Proteobacteria have all been cultured from a number of subsurface marine studies and are also capable of growth on OC substrates (Bowman *et al.*, 2003; D'Hondt *et al.*, 2004; Dang *et al.*, 2009; Yu *et al.*, 2010). Members of the MCG of Archaea have been found in terrestrial and marine subsurface environments, but have not yet been cultured (Inagaki *et al.*, 2003; Fry *et al.*, 2009; Kato *et al.*, 2009; Webster *et al.*, 2010). While sometimes associated with sulfate/methane transition zones, isotopic studies have shown that members of the MCG are capable of both heterotrophic and autotrophic growth (Biddle *et al.*, 2006; Webster *et al.*, 2010). Overall, a mixotrophic, yet dominantly heterotrophic, diverse microbial community in the Ross Sea sediments best explains the large range of $\delta^{13}C_{PLFA}$ values observed, as well as the metabolic capabilities inferred by SSU rRNA sequencing.

CONCLUSIONS

Direct cell count estimates from subglacial sediments beneath the Ross Ice Shelf of Antarctic were as high as 1.7×10^7 cells mL^{-1}, and decreased approximately one order of magnitude within the top 153 cm. Total PLFA concentrations also decrease with depth, ranging from 3.69 to 0.22 nmol g dw^{-1}. Cell density estimates derived from total PLFA concentrations were generally lower but compared well with those derived from AODC. Cell densities from this location are lower than those measured from other near-shore sites and are attributed to low sedimentation rates in this ice-covered environment.

Molecular sequencing of the SSU rRNA gene revealed a diverse community. Surface sediments appear to be more diverse than deeper sediments, although a trend with depth is not apparent. The phylogeny also changes within the core, but not as a function of depth. Instead, the availability of carbon substrates is most likely the factor controlling changes in both phylogeny and the degree of diversity. Stable carbon isotope analyses of PLFAs reveal that most $\delta^{13}C_{PLFAs}$ are depleted approximately 9‰ relative to POC. These $\delta^{13}C$ values are consistent with molecular DNA analyses that collectively suggest a dominantly heterotrophic community.

ACKNOWLEDGMENTS

The authors would like to thank ANDRILL for samples and funding, especially Alex Pyne for his efforts with the push cores. We also like to thank Chuck Pepe-Ranney, Chase Williamson, and Jason Sahl for assistance in the laboratory and with bioinformatics, David Mucciarone for his help with ^{13}C measurements, as well as Chris Mills, Andrew Glossner and Hallgerd Eydal for their editorial comments. We thank our four anonymous reviewers for their thoughtful and very constructive reviews and the editorial handling of Anne Louise Reysenbach and Kurt Konhauser.

REFERENCES

Abraham W-R, Hesse C, Pelz O (1998) Ratios of carbon isotopes in microbial lipids as an indicator of substrate usage. *Applied and Environmental Microbiology* **64**, 4202–4209.

Åkerblom S, Bååth E, Bringmark L, Bringmark E (2007) Experimentally induced effects of heavy metal on microbial activity and community structure of forest mor layers. *Biology and Fertility of Soils* **44**, 79–91.

Albuquerque L, Ferreira C, Tomaz D, Tiago I, Veróssimo A, Da Costa MS, Nobre MF (2009) Meiothermus rufus sp. nov., a new slightly thermophilic red-pigmented species and emended description of the genus Meiothermus. *Systematic and Applied Microbiology* **32**, 306–313.

Allen EE, Facciotti D, Bartlett DH (1999) Monounsaturated but not polyunsaturated fatty acids are required for growth of the deep-sea bacterium *Photobacterium profundum* SS9 at high pressure and low temperature. *Applied and Environmental Microbiology* **65**, 1710–1720.

Altschul SF, Gish W, Miller W, Myers EW, Lipman DJ (1990) Basic local alignment search tool. *Journal of Molecular Biology* **215**, 403–410.

Baker GC, Smith JJ, Cowan DA (2003) Review and re-analysis of domain-specific 16S primers. *Journal of Microbiological Methods* **55**, 541–555.

Ball JW, Mccleskey RB, Nordstrom DK, Holloway JM (2008) Water-chemistry data for slected springs, geyers, and streams in Yellowstone National Park, Wyoming, 2003–005. U.S. Geological Survery Open-File Report 2006-1339, pp. 137.

Beller HR, Letain TE, Chakicherla A, Kane SR, Legler TC, Coleman MA (2006) Whole-genome transcriptional analysis of chemolithoautotrophic thiosulfate oxidation by thiobacillus denitrificans under aerobic versus denitrifying conditions. *Journal of Bacteriology* **188**, 7005–7015.

Bickert T (2000) Influences of geochemical processes on stable isotope distribution in marine sediments. In *Marine*

Geochemistry (eds Schulz HD, Zabel M). Springer, Berlin, pp. 339–362.

Biddle JF, Lipp JS, Lever MA, Lloyd KG, Sørensen KB, Anderson R, Fredricks HF, Elvert M, Kelly TJ, Schrag DP, Sogin ML, Brenchley JE, Teske A, House CH, Hinrichs K-U (2006) Heterotrophic Archaea dominate sedimentary subsurface ecosystems off Peru. *Proceedings of the National Academy of Sciences of the United States of America* **103**, 3846–3851.

Bienhold C, Boetius A, Ramette A (2012) The energy-diversity relationship of complex bacterial communites in Arctic deep-sea sediments. *The ISME Journal* **6**, 724–732.

Blackburn MV, Hannah F, Rogerson A (2009) First account of apochlorotic diatoms from intertidal sand of a south Florida beach. *Estuarine, Coastal and Shelf Science* **84**, 519–526.

Bowman JP, Mccammon SA, Gibson JAE, Robertson L, Nichols PD (2003) Prokaryotic metabolic activity and community structure in antarctic continental shelf sediments. *Applied and Environmental Microbiology* **69**, 2448–2462.

Canfield DE (1994) Factors influencing organic carbon preservation in marine sediments. *Chemical Geology* **114**, 315–329.

Caporaso JG, Bittinger K, Bushman FD, Desantis TZ, Andersen GL, Knight R (2010a) PyNAST: a flexible tool for aligning sequences to a template alignment. *Bioinformatics* **26**, 266–267.

Caporaso JG, Kuczynski J, Stombaugh J, Bittinger K, Bushman FD, Costello EK, Fierer N, González A, Goodrich JK, Gordon JI, Huttley GA, Kelley ST, Knights D, Koenig JE, Ley RE, Lozupone CA, Mcdonald D, Muegge BD, Pirrung M, Reeder J, Sevinsky JR, Turnbaugh PJ, Walters WA, Widmann J, Yatsunenko T, Zaneveld J, Knight R (2010b) QIIME allows analysis of high-throughput community sequencing data. *Nature Methods* **7**, 335–336.

Chao A (1984) Nonparametric estimation of the number of classes in a population. *Scandinavian Journal of Statistics* **11**, 265–270.

Chou Y-M, Polansky AM, Mason RL (1998) Transforming non-normal data to normality in statistical process control. *Journal of Quality Technology* **30**, 133–141.

Coffin RB, Velinsky DJ, Devereux R, Price WA, Cifuentes LA (1990) Stable carbon isotope analysis of nucleic acids to trace sources of dissolved substrates used by estuarine bacteria. *Applied and Environmental Microbiology* **56**, 2012–2020.

Cole JR, Wang Q, Cardenas E, Fish J, Chai B, Farris RJ, Kulam-Syed-Mohideen AS, Mcgarrell DM, Marsh T, Garrity GM, Tiedje JM (2009) The Ribosomal Database Project: improved alignments and new tools for rRNA analysis. *Nucleic Acids Research* **37**, D141–D145.

Cottrell MT, Kirchman DL (2000) Natural assemblages of marine Proteobacteria and members of the Cytophaga-flavobacter cluster consuming low- and high-molecular-weight dissolved organic matter. *Applied and Environment Microbiology* **66**, 1692–1697.

Dang H, Zhu H, Wang J, Li T (2009) Extracellular hydrolytic enzyme screening of culturable heterotrophic bacteria from deep-sea sediments of the Southern Okinawa Trough. *World Journal of Microbiology and Biotechnology* **25**, 71–79.

Danovaro R, Dell'anno A, Corinaldesi C, Magagnini M, Noble R, Tamburini C, Weinbauer MG (2008) Major viral impact on the functioning of benthic deep-sea ecosystems. *Nature* **454**, 1084–1087.

Delong EF, Yayanos AA (1986) Biochemical function and ecological significance of novel bacterial lipids in deep-sea procaryotes. *Applied and Environment Microbiology* **51**, 730–737.

Deming JW, Yager PL, Rowe GT, Pariente V (1992) Natural bacterial assemblages in deep-sea sediments: towards a global view. In *Deep-Sea Food Chains and the Global Carbon Cycle* (eds Rowe GT, Pariente V). Kluwer Academic Publisher, Dordrecht, The Netherlands, pp. 11–27.

D'Hondt S, Rutherford S, Spivack AJ (2002) Metabolic activity of subsurface life in deep-sea sediments. *Science* **295**, 2067–2070.

D'Hondt SL, Jørgensen BB, Miller DJ (2003) *Proc. ODP, Init. Repts., 201.* Ocean Drilling Program, College Station, TX.

D'Hondt S, Jørgensen BB, Miller DJ, Batzke A, Blake R, Cragg BA, Cypionka H, Dickens GR, Ferdelman T, Hinrichs K-U, Holm NG, Mitterer R, Spivack A, Wang G, Bekins B, Engelen B, Ford K, Gettemy G, Rutherford SD, Sass H, Skilbeck CG, Aiello IW, Guèrin G, House CH, Inagaki F, Meister P, Naehr T, Niitsuma S, Parkes RJ, Schippers A, Smith DC, Teske A, Wiegel J, Padilla CN, Acosta JLS (2004) Distributions of microbial activities in deep subseafloor sediments. *Science* **306**, 2216–2221.

D'Hondt S, Spivack AJ, Pockalny R, Ferdelman TG, Fischer JP, Kallmeyer J, Abrams LJ, Smith DC, Graham D, Hasiuk F, Schrum H, Stancin AM (2009) Subseafloor sedimentary life in the South Pacific Gyre. *Proceedings of the National Academy of Sciences* **106**, 11651–11656.

Dodds ED, Mccoy MR, Rea LD, Kennish JM (2005) Gas chromatographic quantification of fatty acid methyl esters: flame ionization detection vs. electron impact mass spectrometry. *Lipids* **40**, 419–428.

Dunbar G, Niessen F, Vogel S, Tulaczyk S, Mandernack K, Krissek L, Carter L, Cowan E, Wilch T, Peng C, Strong CP, Scherer R, Sjunneskog C, Winter D, Mckay R, Talarico F, Pompilio M (2007) Late pleistocence to holocene strata from soft-sediment coring at the AND-1B Site, ANDRILL McMurdo Ice Shelf Project, Antarctica. *Terra Antartica* **14**, 141–154.

Dunstan GA, Volkman JK, Barrett SM, Garland CD (1993a) Changes in the lipid composition and maximisation of the polyunsaturated fatty acid content of three microalgae grown in mass culture. *Journal of Applied Phycology* **5**, 71–83.

Dunstan GA, Volkman JK, Barrett SM, Leroi J-M, Jeffrey SW (1993b) Essential polyunsaturated fatty acids from 14 species of diatom (Bacillariophyceae). *Phytochemistry* **35**, 155–161.

Edgar RC (2010) Search and clustering orders of magnitude faster than BLAST. *Bioinformatics* **26**, 2460–2461.

Expedition 329 Scientists (2011) Expedition 329 summary. In *Proc. IODP, 329* (eds D'Hondt S, Inagaki F, Alvarez Z, Alvarez Zarikian CA, the Expedition 318 Scientist). Integrated Ocean Drilling Program Management International, Inc, Tokyo, pp. 1–61.

Falconer T, Pyne A, Olney M, Curren M, the Andrill-Mis Science Team (2007) Operations overview for the ANDRILL McMurdo Ice Shelf Project, Antarctica. *Terra Antartica* **14**, 131–140.

Fierer N, Bradford MA, Jackson RB (2007) Toward an ecological classification of soil bacteria. *Ecology* **88**, 1354–1364.

Fouilland E, Mostajir B (2010) Revisited phytoplanktonic carbon dependency of heterotrophic bacteria in freshwaters, transitional, coastal and oceanic waters. *FEMS Microbiology Ecology* **73**, 419–429.

Franco MA, De Mesel I, Demba Diallo M, Van Der Gucht K, Van Gansbeke D, Van Rijswijk P, Costa MJ, Vincx M, Vanaverbeke J (2007) Effects of phytoplankton bloom deposition on benthic bacterial communities in two contrasting sediments in the southern North Sea. *Aquatic Microbial Ecology* **48**, 241–254.

Freese E, Rütters H, Köster J, Rullkötter J, Sass H (2009) Gammaproteobacteria as a possible source of eicosapentaenoic acid in anoxic intertidal sediments. *Microbial Ecology* **57**, 444–454.

Fry JC, Horsfield B, Sykes R, Cragg BA, Heywood C, Kim GT, Mangelsdorf K, Mildenhall DC, Rinna J, Vieth A, Zink K-G, Sass H, Weightman AJ, Park JR (2009) Prokaryotic populations and activities in a interbedded coal deposit, including a previously deeply buried section (1.6–2.3 km) above ~150 Ma Basement Rock. *Geomicrobiology Journal* **26**, 163–178.

Gibson GR (1990) Physiology and ecology of the sulphate-reducing bacteria. *Journal of Applied Microbiology* **69**, 769–797.

Gibson DM, Moreau RA, Mcneil GP, Brodie BB (1995) Lipid composition of cyst stages of *Globodera rostochiensis*. *Journal of Nematology* **27**, 304–311.

Goffredi SK, Orphan VJ (2010) Bacterial community shifts in taxa and diversity in response to localized organic loading in the deep sea. *Environmental Microbiology* **12**, 344–363.

Green CT, Scow KM (2000) Analysis of phospholipid fatty acids (PLFA) to characterize microbial communities in aquifers. *Hydrogeology Journal* **8**, 126–141.

Gruber N, Keeling CD, Bacastow RB, Guenther PR, Lueker TJ, Wahlem M, Meijer HAJ, Mook WG, Stocher TF (1999) Spatiotemporal patterns of carbon-13 in the global surface oceans and the oceanic Suess effect. *Global Biogeochemical Cycles* **13**, 307–335.

Guiilini K, Van Oevelen D, Soetaert K, Middelburg JJ, Vanreusel A (2010) Nutritional importance of benthic bacteria for deep-sea nematodes from the Arctic ice margin: results of an isotope tracer experiment. *Limnology and Oceanography* **55**, 1977–1987.

Haack SK, Grachow H, Odelson DA, Forney LJ, Klug MJ (1994) Accuracy, reproducibility, and interpretation of fatty acid methyl ester profiles of model bacterial communities. *Applied and Environmental Microbiology* **60**, 2483–2493.

Harvey HR, Fallon RD, Patton JS (1986) The effect of organic matter and oxygen on the degradation of bacterial membrane lipids in marine sediments. *Geochimica et Cosmochimica Acta* **50**, 795–804.

Hayes JM (2001) Fractionation of carbon and hydrogen isotopes in biosynthetic processes. *Reviews in Mineralogy and Geochemistry* **43**, 225–277.

Hazel JR (1995) Thermal adaptation in biological membranes: is homeoviscous adaption the explanation. *Annual Review of Physiology* **57**, 19–42.

Hinrichs K-U, Inagaki F (2012) Downsizing the deep biosphere. *Science* **338**, 204–205.

Hobbie JE, Daley RJ, Jasper S (1977) Use of nuclepore filters for counting bacteria by fluorescence microscopy. *Applied and Environment Microbiology* **33**, 1225–1228.

House CH, Schopf JW, Stetter KO (2003) Carbon isotopic fractionation by Archaeans and other thermophilic prokaryotes. *Organic Geochemistry* **43**, 345–356.

Inagaki F, Suzuki M, Takai K, Oida H, Sakamoto T, Aoki K, Nealson KH, Horikoshi K (2003) Microbial communities associated with geological horizons in coastal subseafloor sediments from the sea of okhotsk. *Applied and Environment Microbiology* **69**, 7224–7235.

Jagdale GB, Gordon R (1997) Effect of temperature on the composition of fatty acids in total lipids and phospholipids of entomopathogenic nematodes. *Journal of Thermal Biology* **22**, 245–251.

Jiang H, Dong H, Yu B, Liu X, Li Y, Ji S, Zhang CL (2007) Microbial response to salinity change in Lake Chaka, a hypersaline lake on Tibetan plateau. *Environmental Microbiology* **9**, 2603–2621.

Jiao N, Herndl GJ, Hansell DA, Benner R, Kattner G, Wilhelm SW, Kirchman DL, Weinbauer MG, Luo T, Chen F, Azam F (2010) Microbial production of recalcitrant dissolved organic matter: long-term carbon storage in the global ocean. *Nature Reviews. Microbiology* **8**, 593–599.

Jørgensen BB, Boetius A (2007) Feast and famine – microbial life in the deep-sea bed. *Nature Reviews. Microbiology* **5**, 770–781.

Julies EM, Fuchs BM, Arnosti C, Bruchert V (2010) Organic carbon degradation in anoxic organic-rich shelf sediments: biogeochemical rates and microbial abundance. *Geomicrobiology Journal* **27**, 303–314.

Kallmeyer J, Pockalny R, Adhikari RR, Smith DC, D'Hondt S (2012) Global distribution of microbial abundance and biomass in subseafloor sediment. *Proceedings of the National Academy of Sciences* **109**, 16213–16216.

Kato S, Kobayashi C, Kakegawa T, Yamagishi A (2009) Microbial communities in iron-silica-rich microbial mats at deep-sea hydrothermal fields of the Southern Mariana Trough. *Environmental Microbiology* **11**, 2094–2111.

Keil RG (2000) Early diagensis of particulate amino acids in marine sediments. In *Perspectives in Amino Acids and Protein Chemistry* (eds Goodfriend GA, Collins MJ, Fogel ML, Macko SA, Wehmiller JF). Oxford University Press, New York, pp. 69–82.

Koga Y, Morii H (2006) Special methods for the analysis of ether lipid structure and metabolism in archaea. *Analytical Biochemistry* **348**, 1–14.

Lengger SK, Hopmans EC, Sinninghe Damsté JS, Schouten S (2012) Comparison of extraction and work up techniques for analysis of core and intact polar tetraether lipids from sedimentary environments. *Organic Geochemistry* **47**, 34–40.

Lipp JS, Morono Y, Inagaki F, Hinrichs K-U (2008) Significant contribution of Archaea to extant biomass in marine subsurface sediments. *Nature* **454**, 991–994.

Lochte K (1992) Bacterial standing stock and consumption of organic carbon in the benthic boundary layer of the abyssal North Atlantic. In *Deep-Sea Food Chains and the Global Carbon Cycle* (eds Rowe GT, Pariente V). Kluwer Academic Publisher, Dordrecht, The Netherlands, pp. 1–10.

Londry KL, Des Marais DJ (2003) Stable carbon isotope fractionation by sulfate-reducing bacteria. *Applied and Environment Microbiology* **69**, 2942–2949.

Londry KL, Jahnke LL, Des Marais DJ (2004) Stable carbon isotope ratios of lipid biomarkers of sulfate-reducing bacteria. *Applied and Environmental Microbiology* **70**, 745–752.

Ludvigsen L, Albrechtsen HJ, Ringelberg DB, Ekelund F, Christensen TH (1999) Distribution and composition of microbial populations in a landfill leachate contaminated aquifer (Grindsted, Denmark). *Microbial Ecology* **37**, 197–207.

Luna GM, Manini E, Danovaro R (2002) Large fraction of dead and inactive bacteria in coastal marine sediments: comparison of protocols for determination and ecological significance. *Applied and Environmental Microbiology* **68**, 3509–3513.

Manheim FT, Sayles FL (1974) Composition and origin of interstitial waters of marine sediments, based on deep sea drill cores. In *Marine Chemistry. The Sea: Ideas and Observations on Progress in the Study of the Seas* (ed. Goldberg ED). Wiley, New York, pp. 527–568.

Mckay RM, Dunbar GB, Naish TR, Barrett PJ, Carter L, Harper M (2008) Retreat history of the Ross Ice Sheet (Shelf) since the Last Glacial Maximum from deep-basin sediment cores around Ross Island. *Palaeogeography, Palaeoclimatology, Palaeoecology* **260**, 245–261.

Mills CT, Dias RF, Graham D, Mandernack KW (2006) Determination of phospholipid fatty acid structure and stable carbon isotope composition of deep-sea sediments of the Northwest Pacific, ODP site 1179. *Marine Chemistry* **98**, 197–209.

Mills HJ, Hunter E, Humphrys M, Kerkhof L, Mcguinness L, Huettel M, Kostka JE (2008) Characterization of nitrifying, denitrifying, and overall bacterial communities in permeable marine sediments of the Northeastern Gulf of Mexico. *Applied and Environment Microbiology* **74**, 4440–4453.

Mills CT, Amano Y, Slater GF, Dias RF, Iwatsuki T, Mandernack KW (2010) Microbial carbon cycling in oligotrophic regional aquifers near the Tono Uranium Mine, Japan as inferred from δ13C and Δ14 of in situ phospholipid fatty acids and carbon sources. *Geochimica et Cosmochimica Acta* **74**, 3785–3805.

Miroshnichenko ML, L'haridon S, Nercessian O, Antipov AN, Kostrikina NA, Tindall BJ, Schumann P, Spring S, Stackebrandt E, Bonch-Osmolovskaya EA, Jeanthon C (2003) Vulcanithermus mediatlanticus gen. nov., sp. nov., a novel member of the family Thermaceae from a deep-sea hot vent. *International Journal of Systematic and Evolutionary Microbiology* **53**, 1143–1148.

Morin RH, Williams T, Henrys SA, Marens D, Niessen F, Hansarak D (2010) Heat flow and hydrologic characteristics at the AND-1B borehole, ANDRILL McMurdo Ice Shelf Project, Antarctica. *Geosphere* **6**, 370–378.

Morono Y, Terada T, Masui N, Inagaki F (2009) Discriminative detection and enumeration of microbial life in marine subsurface sediments. *The ISME Journal* **3**, 503–511.

Moy CM, Dunbar RB, Moreno PI, Francois J-P, Villa-Martínez R, Mucciarone DM, Guilderson TP, Garreaud R (2008) Isotopic evidence for hydrologic change related to the westerlies in SW Patagonia, Chile, during the last millennium. *Quaternary Science Reviews* **27**, 1335–1349.

Naish T, Powell R, Levy R, Wilson G, Scherer R, Talarico F, Krissek L, Niessen F, Pompilio M, Wilson T, Carter L, Deconto R, Huybers P, Mckay R, Pollard D, Ross J, Winter D, Barrett P, Browne G, Cody R, Cowan E, Crampton J, Dunbar G, Dunbar N, Florindo F, Gebhardt C, Graham I, Hannah M, Hansaraj D, Harwood D, Helling D, Henrys S, Hinnov L, Kuhn G, Kyle P, Läufer A, Maffioli P, Magens D, Mandernack K, Mcintosh W, Millan C, Morin R, Ohneiser C, Paulsen T, Persico D, Raine I, Reed J, Riesselman C, Sagnotti L, Schmitt D, Sjunneskog C, Strong P, Taviani M, Vogel S, Wilch T, Williams T (2009) Obliquity-paced Pliocene West Antarctic ice sheet oscillations. *Nature* **458**, 322–328.

Nichols DS, Brown JL, Nichols PD, Mcmeekin TA (1997) Production of eicosapentaenoic and arachidonic acids by an antarctic bacterium: response to growth temperature. *FEMS Microbiology Ecology* **152**, 349–354.

Nishihara M, Koga Y (1987) Extraction and composition of polar lipids from the Archaebacterium, *Methanobacterium thermoautotrophicum*: effective extraction of tetraether lipids by an acidified solvent. *Journal of Biochemistry* **101**, 997–1005.

Nobre MF, Trüper H, Da Costa MS (1996) Transfer of *Thermus ruber* (Loginova et al. 1984), *Thermus silvanus* (Tenreiro et al. 1995), and *Thermus chliarophilus* (Tenreiro et al. 1995) to *Meiothermus* gen. nov. as *Meiothermus ruber* comb. nov., *Meiothermus silvanus* comb. nov., and *Meiothermus chliarophilus* comb. nov., respectively, and emendation of the genus Thermus. *International Journal of Systematic Bacteriology* **46**, 604–606.

Oakes JM, Eryre BD, Middleburg JJ, Boschker HTS (2010) Composition, production, and loss of carbohydrates in subtropical shallow subtidal sandy sediemnts: rapid processing and long-term retention revealed by ^{13}C-labeling. *Limnology and Oceanography* **55**, 2126–2138.

Pancost RD, Sinninghe Damsté JS (2003) Carbon isotopic compositions of prokaryotic lipids as tracers of carbon cycling in diverse settings. *Chemical Geology* **195**, 29–58.

Parkes RJ, Cragg BA, Wellsbury P (2000) Recent studies on bacterial populations and processes in subseafloor sediments: a review. *Hydrogeology Journal* **8**, 11–28.

Parkes RJ, Webster G, Cragg BA, Weightman AJ, Newberry CJ, Ferdelman TG, Kallmeyer J, Jørgensen BB, Aiello IW, Fry JC (2005) Deep sub-seafloor prokaryotes stimulated at interfaces over geological time. *Nature* **436**, 390–394.

Parkes RJ, Cragg BA, Banning N, Brock F, Webster G, Fry JC, Hornibrook E, Pancost RD, Kelly S, Knab N, Jørgensen BB, Rinna J, Weightman AJ (2007) Biogeochemistry and biodiversity of methane cycling in subsurface marine sediments (Skagerrak, Denmark). *Environmental Microbiology* **9**, 1146–1161.

Pompilio M, Dunbar N, Gebhardt AC, Helling D, Kuhn G, Kyle P, Mckay R, Talarico F, Tulaczyk S, Vogel S, Wilch T (2007) Petrology and geochemistry of AND-1B Core, ANDRILL McMurdo Ice Chelf Project, Antarctica. *Terra Antartica* **3**, 255–288.

Preuss A, Schauder R, Fuchs G, Stichler W (1989) Carbon isotope fracationation by autotrophic bacteria with three different CO_2 fixation pathways. *Zeitschrift fur Naturforschung* **44c**, 397–402.

Pruesse E, Quast C, Knittel K, Fuchs BM, Ludwig W, Peplies J, Glöckner FO (2007) SILVA: a comprehensive online resource for quality checked and aligned ribosomal RNA sequence data compatible with ARB. *Nucleic Acids Research* **35**, 7188–7196.

Rublee P (1982) *Bacteria and Microbial Distribution in Estuarine Sediments*. Academic Press, Inc., New York.

Rütters H, Sass H, Cypionka H, Rullkötter J (2002) Microbial communities in a Wadden Sea sediment core–clues from analyses of intact glyceride lipids, and released fatty acids. *Organic Geochemistry* **33**, 803–816.

Schouten S, Strous M, Kuypers M, Rijpstra WIC, Baas M, Schubert CJ, Jetten MSM, Sinninghe Damsté JS (2004) Stable carbon isotopic fractionations associated with inorganic carbon fixation by anaerobic ammonium-oxidizing bacteria. *Applied and Environmental Microbiology* **70**, 3785–3788.

Shannon CE, Weaver W (1949) *The Mathematical Theory of Communication*. The University of Illinois Press, Urbana, IL.

Shipboard Scientific Party (2003) Leg 201 summary. In *Proc. ODP, Init. Repts., 201* (eds D'Hondt S, Jørgensen BB, Miller DJ). Ocean Drilling Program, College Station, TX, pp. 1–81.

Smith DC, D'Hondt S (2006) Exploration of life in deep subseafloor sediments. *Oceanography* **19**, 60–72.

Summit MP, Ringelberg DB, White DC, Baross J (2000) Phospholipid fatty acid-derived microbial biomass and community dynamics in hot, hydrothermally influenced sediments form Middle Valley, Juan De Fuca Ridge. In *Proceedings of the Ocean Drilling Program, Scientific Results* (eds Zierenberg RA, Fouquet Y, Miller DJ, Normark WR). Ocean Drilling Program, College Station, TX, pp. 1–19.

Teece MA, Fogel ML, Dollhopf ME, Nealson KH (1999) Isotopic fractionation associated with biosynthesis of fatty acids by a marine bacterium under oxic and anoxic conditions. *Organic Geochemistry* **30**, 1571–1579.

Tornabene TG, Kates M, Volcani BE (1974) Sterols, aliphatic hydrocarbons, and fatty acids of a nonphotosynthetic diatom, *Nitzschia alba*. *Lipids* **9**, 279–284.

Vetriani C, Jannasch HW, Macgregor BJ, Stahl DA, Reysenbach A-L (1999) Population structure and phylogenetic characterization of marine benthic archaea in deep-sea sediments. *Applied and Environment Microbiology* **65**, 4375–4384.

Volkman JK, Barrett SM, Blackburn SI, Mansour MP, Sikes EL, Gelin F (1998) Microalgal biomarkers: a review of recent research developments. *Organic Geochemistry* **29**, 1163–1179.

Wakeham SG, Lee C, Hedges JI, Hernes PJ, Peterson MJ (1997) Molecular indicators of diagenetic status in marine organic matter. *Geochimica et Cosmochimica Acta* **61**, 5363–5369.

Webster G, Rinna J, Roussel EG, Fry JC, Weightman AJ, Parkes RJ (2010) Prokaryotic functional diversity in different biogeochemical depth zones in tidal sediments of the Severn Estuary, UK, revealed by stable-isotope probing. *FEMS Microbiology Ecology* **72**, 179–197.

White DC, Ringelberg DB (1998) Signature lipid biomarker analysis. In *Techniques in Microbial Ecology* (eds Burlage RS, Atlas R, Stahl D, Geesey G, Sayler G). Oxford University Press, New York, pp. 225–271.

White DC, Bobbie RJ, Herron JS, King JD, Morrison SL (1979) Biochemical measurements of microbial biomass and activity from environmental samples. In *Native Aquatic Bacteria: Enumeration, Activity and Ecology* (eds Costerton JW, Colwell RR). American Society for Testing and Materials, Philadelphia, PA, pp. 69–81.

Whitman WB, Coleman DC, Wiebe WJ (1998) Prokaryotes: the unseen majority. *Proceedings of the National Academy of Sciences of the United States of America* **95**, 6578–6583.

Yamada T, Sekiguchi Y (2009) Cultivation of uncultured Chloroflexi subphyla: significance and ecophysiology of formerly uncultured Chloroflexi 'Subphylum I' with natural and biotechnological relevance. *Microbes and Environments* **24**, 205–216.

Yamada T, Sekiguchi Y, Hanada S, Imachi H, Ohashi A, Harada H, Kamagata Y (2006) *Anaerolinea thermolimosa* sp. nov., *Levilinea saccharolytica* gen. nov., sp. nov. and *Leptolinea tardivitalis* gen. nov., sp. nov., novel filamentous anaerobes, and description of the new classes *Anaerolineae classis* nov. and *Caldilineae classis* nov. in the bacterial phylum Chloroflexi. *International Journal of Systematic and Evolutionary Microbiology* **56**, 1331–1340.

Yoon D-N, Park S-J, Kim S-J, Jeon C, Chae J-C, Rhee S-K (2010) Isolation, characterization, and abundance of filamentous members of Caldilineae in activated sludge. *Journal of Microbiology* **48**, 275–283.

Yu Y, Li H, Zeng Y, Chen B (2010) Phylogenetic diversity of culturable bacteria from Antarctic sandy intertidal sediments. *Polar Biology* **33**, 869–875.

Zhang CL, Li Y, Fong JB, Peacock AD, Blunt E, Fang J, Lovley DR, White DC (2003) Carbon isotope signatures of fatty acids in *Geobacter metallireducens* and *Shewanella algae*. *Chemical Geology* **195**, 17–28.

Zhang C, Fouke BE, Bonheyo GT, Peacock AD, White DC, Huang Y, Romanek CS (2004) Lipid biomarkers and carbon-isotopes of modern travertine deposits (Yellowstone National Park, USA): implication for biogeochemical dynamics in hot-spring systems. *Geochimica et Cosmochimica Acta* **68**, 3157–3169.

SUPPORTING INFORMATION

Additional Supporting Information may be found in the online version of this article:

Table S1. A summary of reported cell densities from various oceanic microbial studies.